

# Lawrence Berkeley National Laboratory

## Recent Work

### Title

NMR DETERMINATIONS OF BARRIERS TO INTERNAL ROTATION IN HALOGEN SUBSTITUTED ETHANES

### Permalink

<https://escholarship.org/uc/item/1s97j0jq>

### Authors

Newmark, Richard A.  
Sederholm, C.H.

### Publication Date

1965-02-01

**University of California**  
**Ernest O. Lawrence**  
**Radiation Laboratory**

**TWO-WEEK LOAN COPY**

*This is a Library Circulating Copy  
which may be borrowed for two weeks.  
For a personal retention copy, call  
Tech. Info. Division, Ext. 5545*

**NMR DETERMINATIONS OF BARRIERS TO INTERNAL  
ROTATION IN HALOGEN SUBSTITUTED ETHANES**

**Berkeley, California**

## **DISCLAIMER**

This document was prepared as an account of work sponsored by the United States Government. While this document is believed to contain correct information, neither the United States Government nor any agency thereof, nor the Regents of the University of California, nor any of their employees, makes any warranty, express or implied, or assumes any legal responsibility for the accuracy, completeness, or usefulness of any information, apparatus, product, or process disclosed, or represents that its use would not infringe privately owned rights. Reference herein to any specific commercial product, process, or service by its trade name, trademark, manufacturer, or otherwise, does not necessarily constitute or imply its endorsement, recommendation, or favoring by the United States Government or any agency thereof, or the Regents of the University of California. The views and opinions of authors expressed herein do not necessarily state or reflect those of the United States Government or any agency thereof or the Regents of the University of California.

UNIVERSITY OF CALIFORNIA  
Lawrence Radiation Laboratory  
Berkeley, California

AEC Contract No. W-7405-eng-48

NMR DETERMINATIONS OF BARRIERS TO  
INTERNAL ROTATION IN HALOGEN SUBSTITUTED ETHANES

Richard A. Newmark and C. H. Sederholm

February, 1965

NMR Determinations of Barriers to  
Internal Rotation in Halogen Substituted Ethanes

Richard A. Newmark<sup>‡</sup> and C. H. Sederholm

Inorganic Materials Research Division,  
Lawrence Radiation Laboratory and  
Department of Chemistry, College of Chemistry,  
University of California  
Berkeley, California

Abstract

The theory of Kaplan and Alexander for exchange in nuclear magnetic resonance (NMR) systems has been applied to exchange between three species with any number of nuclei of spin  $\frac{1}{2}$ , in which all the nuclei in each species are exchanged by the interconversion. A set of explicit equations for the density matrix elements in this case is written down. Computer programs have been written to solve the equations in the two and three spin cases. The results enable the calculation of NMR spectra of highly coupled nuclei undergoing exchange. Absolute reaction rate theory has been used to express the rates of exchange in terms of activation energies. This has been combined with the Kaplan-Alexander theory to determine the

---

<sup>‡</sup> National Science Foundation Predoctoral Fellow, 1961-1964.  
Present address: Department of Chemistry, Massachusetts Institute  
of Technology, Cambridge, Massachusetts, 02139.

free energies of activation for internal rotation in several halogenated ethanes,  $\text{CFCl}_2\text{-CFCl}_2$ ,  $\text{CF}_2\text{Br-CCl}_2\text{Br}$ ,  $\text{CF}_2\text{Br-CFBr}_2$ ,  $\text{CF}_2\text{Br-CFBrCl}$ ,  $\text{CFClBr-CFClBr}$ , and  $\text{CF}_2\text{Br-CHBrCl}$ . Spectra were calculated assuming limiting values for the transmission coefficient,  $K \ll 1$ ,  $K = 1$ . The first case implies free rotation occurs when a molecule is excited to sufficient energy to exceed the barriers. Alternatively, the second case implies that deactivation of the rotational mode occurs in a time comparable with the rotational frequency. The experimental results on  $\text{CF}_2\text{Br-CCl}_2\text{Br}$  can only be explained by the second possibility. The barriers are discussed in terms of the distortion necessary to form the activated complex in which the substituents are eclipsed.

The low temperature spectrum of the three rotamers of  $\text{CF}_2\text{Br-CHBrCl}$  shows two large vicinal HF coupling constants (18 cps) and four small ones (less than 3 cps). The assignment of the rotamers made assuming that the low barrier observed between two of the rotamers does not involve eclipsing two large halogens indicates that the large coupling constants are trans and the four others are gauche coupling constants.

## I. Introduction

Much work has been done to measure the barriers to internal rotation in substituted ethanes, as is indicated by Wilson's recent review of the subject.<sup>1</sup> Extensive microwave studies of substituted ethanes containing a methyl group indicate the barrier is near 3 kcal/mole in all of these compounds. Infrared and electron diffraction measurements have yielded larger barriers of 4.2 and 10.8 kcal/mole in the symmetrical molecules hexafluoroethane<sup>2</sup> and hexachloroethane,<sup>3</sup> respectively. From infrared and Raman spectral studies<sup>4,5</sup> intermediate barriers have been reported for several molecules containing a  $CF_3$  group on one end. To obtain the barrier from microwave or infrared data for an asymmetric top on an asymmetric framework is very difficult. Halogenated ethanes containing fluorine in which the barriers are above roughly 6 kcal/mole lend themselves to investigation by nuclear magnetic resonance (NMR). This extends the type of molecules which can be conveniently studied to totally asymmetric cases.

## II. Theory of Exchange

The free energies of activation for the internal rotation of  $CFClBr-CFClBr$  have been determined previously by NMR measurements.<sup>6</sup> The Bloch equation, as modified by McConnell,<sup>7</sup> in conjunction with absolute reaction rate theory were used to calculate the spectra. Free energies of activation, which will be termed for convenience the barriers to internal rotation although the two are not exactly the same, were obtained assuming a transmission coefficient near unity. The Bloch-McConnell equations provide suitable results when the coupling constants

may be neglected. However, to extend the analysis to other perhalogenated ethanes, such as  $\text{CF}_2\text{Br-CBrClX}$ ,  $X = \text{H, F, and Cl}$ , in which the coupling constant between the geminal fluorines is almost as large as the chemical shift, it is necessary to use a theory of exchange among nuclei in different environments which includes the coupling. Kaplan<sup>8</sup> developed such a theory based on the self-consistent averaged density matrix of the spin system. Alexander,<sup>9</sup> from a suggestion by Kaplan,<sup>10</sup> developed a similar set of equations by deriving a Boltzmann equation for the average density matrix elements. Kurland and Wise,<sup>11</sup> and Heidberg et al.<sup>12</sup> have used the theory of Alexander to study hindered internal rotation between identical systems for two spin systems. We have extended the theory to calculate spectra of three species undergoing exchange, and applied it to obtain barriers in molecules exhibiting AB and ABX spectra.

Internal rotation is an exchange process which can be treated by the above theories for intermolecular exchange. At equilibrium, in which the average effect is studied, the exchange of two rotamers is indistinguishable from the actual physical process in which A transforms (or rotates) to B while, to preserve equilibrium, some other species (or rotamer) B transforms to A. This argument invalidates Johnson's claim that internal rotation in which the nuclei change their environments cannot be treated by Alexander's theory.<sup>13</sup> The equations given by Johnson for internal rotation from a modification of Kubo's theory are identical to those derived below from Alexander's theory.

The exchange operator  $P$  is defined such that  $\psi(t) \rightarrow P \psi(t)$  whenever an exchange occurs. If we denote the product wave function of one species of  $N$  spins by  $i_1 i_2 \dots i_N$ , where  $i_k$  is an eigenfunction of the



z component of angular momentum for nucleus k, and the product wave function of the second species by  $j_1 j_2 \dots j_N$ , then under exchange we have

$$P \phi (i_1 i_2 \dots i_N; j_1 j_2 \dots j_N) = \phi (j_1 j_2 \dots j_N; i_1 i_2 \dots i_N). \quad (1)$$

If  $\psi$  is a linear combination of product wave functions,  $\psi_j = \sum_k a_{jk} \phi_k$ , then  $P\psi$  is a similar linear combination and the matrix representation of  $P$  will be a function of the  $a_{jk}$  for the two species involved in the exchange. The effect of the exchange between two species A and B carries the interaction density matrix  $\rho^A \cdot \rho^B$  into  $P^{AB} \rho^A \cdot \rho^B (P^{AB})^{-1}$ .

Kaplan's theory<sup>8</sup> has been used to develop an explicit set of simultaneous equations for the density matrix elements in the representation in which the time-independent NMR Hamiltonian for each species is diagonal.<sup>14</sup> In this representation, which is used to conveniently represent the time-dependence of the density matrix after exchange, the form of the exchange matrix is a product of the unitary matrices,  $a_{ij}^L$  which diagonalize the Hamiltonian for species L. Thus,

$$P_{ij,kl}^{AB} = \sum_q a_{iq}^A a_{kq}^B \sum_r a_{jr}^A a_{lr}^B, \quad (2)$$

where the first pair of subscripts of  $P$  denotes the row and the second pair the column.

Most of the calculations were performed using a computer program written from Kaplan's theory.<sup>14</sup> However, identical results can be obtained from the set of simultaneous equations which arise from the theory given in detail by Alexander, and the resulting equations are more readily generalized to more complex systems. The main simplification is that the representation of the product wave functions can be used. In this

representation the exchange matrix takes the simpler form,

$$P_{ij,kl}^{AB} = \delta_{il} \delta_{jk} \quad (3)$$

where  $\delta_{ij}$  is 1 if the subscripts are equal and zero otherwise.

In the case of internal rotation of ethanes Alexander's theory<sup>9b</sup> is extended to the three pairwise exchanges between the three species A, B, and C by introducing a term for the AC exchange as well as the AB exchange in the equation for the time development of the density matrix due to exchange,

$$\left(\frac{d\rho^A}{dt}\right)_{\text{exch}} = \frac{\tau_A}{\tau_{AB}} \Omega^B (P^{AB} \rho^A P^{AB}) + \frac{\tau_A}{\tau_{AC}} \Omega^C (P^{AC} \rho^A P^{AC}) - \rho^A \quad (4)$$

$P^{AB}$  and  $P^{AC}$  are the orthogonal matrices for the AB and AC exchange, respectively.  $\Omega^B$  and  $\Omega^C$  are contraction operators which describe averaging over all elements diagonal in the spin function of B or C to yield the density matrix for species A after the exchange.  $\tau_A$  is the correlation time for species A, given by

$$\frac{1}{\tau_A} = \frac{1}{\tau_{AB}} + \frac{1}{\tau_{AC}} \quad (5)$$

where  $\tau_{AB}$  is the correlation time for the AB exchange. Thus  $\tau_A/\tau_{AB}$  and  $\tau_A/\tau_{AC}$  are normalized weighting factors corresponding to the probability of an AB or an AC exchange.

For the particular case of exchange between two rotamers all the spins of one rotamer are exchanged with all the spins of the other. This eliminates all the summations and the term due to the nonexchanging nuclei

in Eq. (20) of Alexander<sup>9b</sup> for the time-dependence of the off-diagonal density matrix elements in the rotating coordinate system. Including an additional term from Eq. (4) above for the AC exchange, Alexander's equation becomes,

$$\begin{aligned} \langle j | \frac{d\rho^A}{dt} | k \rangle &= \frac{\langle j | \rho^B | k \rangle}{\tau_{AB}} + \frac{\langle j | \rho^C | k \rangle}{\tau_{AC}} - \left[ \frac{1}{\tau_A} + \frac{1}{T_{2A}} \right] \langle j | \rho^A | k \rangle \\ &+ i \langle j | [\rho^A, H^A] | k \rangle + i \langle j | [\rho^A, H_1 I_x^A] | k \rangle. \end{aligned} \quad (6)$$

$H^A$  is the time independent Hamiltonian in the coordinate system rotating at the frequency,  $\omega = 2\pi\nu$ , of the applied rf field,

$$H^A = \sum_m (\nu_m^A - \nu) I_{zm}^A + \sum_{m>n} J_{mn}^A \vec{I}_m^A \cdot \vec{I}_n^A, \quad (7)$$

where  $\nu_m^A$  is the chemical shift of nucleus  $m$  in rotamer  $A$  and  $J$  is the coupling constant. The term  $\frac{1}{T_{2A}} \langle j | \rho^A | k \rangle$  introduces the phenomenological transverse relaxation time  $T_2$ , such that the equations reduce to the Bloch equations in the absence of exchange.  $H_1$  is the magnitude of the rf field in cps, and the last term in Eq. (6) may be reduced to  $i D \langle j | I_x^A | k \rangle$  to first order in  $\frac{\hbar\omega_0}{kT}$  where  $D = \gamma H_1 \omega_0 / kT$  and  $\omega_0 = \gamma H_0$  is the Larmor frequency,<sup>9a</sup>  $\hbar$  is Planck's constant divided by  $2\pi$ ,  $k$  the Boltzmann constant, and  $T$  the temperature. Equations for  $\frac{d\rho^B}{dt}$  and  $\frac{d\rho^C}{dt}$  are obtained by a cyclic permutation of the indices  $A, B$ , and  $C$ .

Finally, the absorption is given by the imaginary part of the expectation value of the transverse component of the angular momentum,

$$\text{Im} \langle I_x + iI_y \rangle = \text{ImTr}[(I_x + iI_y)\rho] = \sum_{m,n} (I_x + iI_y)_{mn} \text{Im} \rho_{nm} \quad (8)$$

(The dispersion is given by the real part of the expectation value.)

One must only solve Eq. (6) for those density matrix elements which contribute to the absorption in Eq. (8). Thus, the only elements which concern us in Eq. (6) are those in which state  $j$  differs from state  $k$  by  $+1$  in the  $z$  component of the angular momentum.

Under unsaturated steady state conditions the time derivatives in Eq. (6) are set equal to zero, leaving a set of simultaneous equations with complex coefficients. These can be considerably simplified and reduced to a set of real equations by the following considerations:

We define a doubly subscripted vector,  $\rho_{mn}$ , such that  $m$  refers to the rotamer, (1, 2, and 3 for A, B, and C) and  $n$  refers to one of the spin product wave functions of interest. To evaluate the fourth term in Eq. (6), note that  $H^A|k\rangle = \sum_m a_{km}^A |m\rangle$  where the  $z$  component of the angular momentum of state  $|m\rangle$  must be the same as that of  $|k\rangle$  since  $F_z^A = \sum_m I_{zm}^A$  is a good quantum number. Thus,

$$\langle j | [\rho^A, H^A] | k \rangle = \sum_m [a_{km}^A \langle j | \rho^A | m \rangle - a_{jm}^A \langle m | \rho^A | k \rangle], \quad (9)$$

where  $a_{ij}^A$  is a real function of the coupling constants and chemical shifts for rotamer A.

Eq. (6) for  $d\rho_{ln}/dt$  now becomes

$$0 = \frac{\rho_{2n}}{\tau_{AB}} + \frac{\rho_{3n}}{\tau_{AC}} - \rho_{ln} \left[ \frac{1}{\tau_A} + \frac{1}{T_{2A}} \right] + i \sum_m b_{lm} \rho_{lm} + iD(I_x)_{lm}, \quad (10)$$

where the  $b_{lm}$  may be determined from Eq. (9). Because  $F_z^A$  is a good quantum number there is no coupling between density matrix elements of the different rotamers which do not have the same change in  $F_z^L$ . Thus, if there are an even number of spins, the elements for the  $F_z^L = 1$  to  $F_z^L = 0$  transitions do not couple to those for the  $F_z^L = 0$  to  $F_z^L = -1$  transitions, etc.

Including similar equations for  $dp_{2n}/dt$  and  $dp_{3n}/dt$ , we can write a matrix equation for the vector  $\vec{\rho}$  as:

$$(\tilde{A} + i\tilde{\alpha} + iv\tilde{I})\vec{\rho} = -iD\vec{I}_x. \quad (11)$$

$\tilde{A}$  is a real matrix comprising the correlation and relaxation time terms in Eq. (10). The  $i\tilde{\alpha} + iv\tilde{I}$  terms arise from the matrix elements of the commutator in Eq. (6), where  $\tilde{I}$  is the unit matrix. The contribution of the term  $\sum_m (-v) I_{zm}^L$  in Eq. (7) to  $\langle j | [\rho^L, H^L] | k \rangle$  is  $v \langle j | \rho^L | k \rangle$ , for  $L = A, B, \text{ or } C$ . This gives the  $iv\tilde{I}$  term. The  $i\tilde{\alpha}$  term arises from the contribution of the remaining part of  $H^L$ ;  $\tilde{\alpha}$  is also a real matrix since  $H^L$  is real.

Since we are only interested in the imaginary part of  $\vec{\rho}$ , we set  $\vec{\rho} = \vec{u} + i\vec{v}$ , where  $\vec{u}$  and  $\vec{v}$  are real vectors. Substituting into Eq. (11) and equating the real and imaginary parts gives two matrix equations for  $\vec{u}$  and  $\vec{v}$ . Eliminating  $\vec{u}$  and solving for  $\vec{v}$  yields

$$\tilde{E} \vec{v} = (\tilde{\alpha} A^{-1} \tilde{\alpha} + \tilde{A} + v(\tilde{\alpha} A^{-1} + A^{-1} \tilde{\alpha}) + v^2 A^{-1}) \vec{v} = D \vec{I}_x. \quad (12)$$

Since  $\rho_{2m}$  and  $\rho_{3m}$  do not enter the equation for  $dp_{1n}/dt$  if  $m \neq n$ , the matrix  $A$  has the form  $A_{ij,km} = B_{ik} \delta_{jm}$ , where  $B_{ik}$  is the  $3 \times 3$  matrix,

$$\begin{pmatrix} -\tau_A^{-1} - T_{2A}^{-1} & \tau_{AB}^{-1} & \tau_{AC}^{-1} \\ \tau_{BA}^{-1} & -\tau_B^{-1} - T_{2B}^{-1} & \tau_{BC}^{-1} \\ \tau_{CA}^{-1} & \tau_{CB}^{-1} & -\tau_C^{-1} - T_{2C}^{-1} \end{pmatrix}$$

$\tilde{\alpha}$  is clearly diagonal in blocks for each rotamer,  $\alpha_{ij,km} = \delta_{ik} Y_{jm}^i$ .

Making the above substitutions into Eq. (12) gives the matrix elements of  $\tilde{E}$ ,

$$E_{ij,km} = B_{ik} \delta_{jm} + \sum_n Y_{jn}^i B_{ik}^{-1} Y_{nm}^k + \nu B_{ik}^{-1} (Y_{jm}^i + Y_{jm}^k) + \nu^2 B_{ik}^{-1} \delta_{jm} \quad (13)$$

In order to calculate spectra the set of simultaneous equations (12) are solved for the  $\nu_{nm}$  and the absorption obtained directly from Eq. (8). Computer programs have been written to calculate spectra for three rotamers with AB or ABX spectra undergoing exchange.<sup>15</sup> It is easy to extend the programs to more complex systems.

From absolute reaction rate theory,<sup>16</sup> the rate of exchange between rotamers i and j is given by

$$k_{ij} = \kappa \frac{kT}{h} e^{-\Delta F^\ddagger/RT} \quad (14)$$

where  $\Delta F^\ddagger$  is the free energy of activation and  $\kappa$  is the transmission coefficient, defined as the rate of formation of deactivated product molecules produced by crossing the barrier under consideration divided by the rate of molecules crossing the barrier.

Two limiting values of the transmission coefficient,  $\kappa$ , corresponding to two deactivation models are considered. If one assumes that deactivation of the torsional mode of a molecule is very slow compared to the torsional frequency, then  $\kappa \ll 1$ , and the resulting rate expressions are independent of the highest barrier. Consider a potential curve as in Fig. 1. If a rotamer in the potential minimum  $E_1$  were excited with sufficient energy to exceed barrier  $E_6$ , but not  $E_5$ , it would remain in the excited state for a sufficiently long time to perform several torsional vibrations in the large well bounded by barriers  $E_4$  and  $E_5$ . It would then have equal probability of falling into potential wells.

$E_1$  or  $E_2$ . If the original excitation energy had been greater than  $E_5$  but less than  $E_4$ , the molecule would perform several torsional vibrations in the large well bounded by  $E_4$  on either side, and would finally have equal probability of falling into each of the three potential minima. As the excitation energy exceeds  $E_4$  the motion while in the excited state would become a free rotation rather than a torsional vibration. However, the probability of falling into any one minimum would still be the same, namely one third. Hence, the rates are independent of the highest barrier,  $E_4$ , since interchange between any two rotamers is possible whenever the molecule's energy exceeds  $E_5$ .

On the other hand, if deactivation of the torsional mode occurs almost immediately after a molecule passes over one of the maxima, then  $\chi = 1$ , and the rate expressions are a function of the highest barrier; in fact, the rate between any two potential minimum depends only on the barrier height between them. In this case the six rates are given by

$$k_{ij} = \frac{kT}{h} e^{-(F_{ij}^\ddagger - F_i)/RT}, \quad (15)$$

$i = 1$  to  $3$ ,  $j = 1$  to  $3$ , and  $i \neq j$ .  $F_i$  is the free energy of the potential minimum and  $F_{ij}^\ddagger$  is the free energy of the activated complex, both measured from the energy of the potential minimum of the most stable rotamer,  $F_1 = 0$ .

Since the assumption that  $\chi \ll 1$  leads to one fewer arbitrary parameters to be used in matching the experimental with the calculated spectra, this assumption was originally made. However, it was then impossible to duplicate the experimental spectra of  $\text{CF}_2\text{Br}-\text{CCl}_2\text{Br}$ . For this molecule, configurations 2 and 3 are identical, and  $E_4$  and

$E_6$  are identical barriers by symmetry. Setting barrier  $E_5$  to any value less than or equal to  $E_4$  does not yield the observed spectra. These results will be described in detail in the section on  $\text{CF}_2\text{Br}-\text{CCl}_2\text{Br}$ .

In addition to this experimental data, the following theoretical argument implies that the assumption  $K = 1$  is probably more reasonable.

Classically, the angular velocity of rotation,  $\omega$ , can be calculated from the kinetic energy,  $K_E$ , by

$$K_E = \frac{1}{2} \omega I^2. \quad (16)$$

At the temperature of these experiments the median energy of the molecules above a barrier is about .3 kcal/mole above the barrier. The moment of inertia,  $I$ , about the axis of rotation is roughly  $1 \times 10^{-37}$  gm  $\text{cm}^2$  for any perhalogenated ethane. The angular velocity is much faster when a molecule is in the staggered configuration and possesses mostly kinetic energy. Approximating the potential function in Figure 1 by three square wells, it is seen that the molecule spends half of its time with a small kinetic energy and the other half with a larger kinetic energy. Therefore the angular velocity calculated from Eq. (16) with  $K_E = 0.3$  kcal./mole is the rate for roughly half of the revolution while the other half revolution takes place much more rapidly. With these approximations, the average angular velocity is  $1 \times 10^{12}$  radians per second.

The primary source of deactivation in solution is collisions, so it is necessary to compare the collision rate with the angular velocity. Frost and Pearson<sup>17</sup> justify using elementary collision theory to calculate frequency factors for reactions in solution. The number of



collisions per second,  $Z_A$ , is given by

$$Z_A = \left( \frac{8\pi kT}{\mu} \right)^{\frac{1}{2}} \sigma_{AB}^2 n_B \quad (17)$$

The calculation was performed for one molecule of  $\text{CF}_2\text{Br}-\text{CCl}_2\text{Br}$  (M.W.=293) in  $\text{CFCl}_3$ . The density of the solvent,  $n_B$ , is 1.49 gm/cc.  $\sigma_{AB}$  is the mean radius of A and B, taken as 4 Å, and  $\mu$  is the reduced mass. The number of collisions/second is  $1 \times 10^{12}$ . Although this provides an order of magnitude result, Benson<sup>18</sup> points out that if one chooses a reasonable interaction potential between molecules in a solution, such as the hard sphere well model, then the potential energy of interaction between a molecule with its 4 to 12 nearest neighbors is always of the order of magnitude of  $kT$  (thermal energy).

Consequently, it is not unreasonable to assume that deactivation occurs immediately following a rotation. Cagle and Eyring<sup>19</sup> have shown this to be true for internal rotation of substituted biphenyls in the liquid phase. If  $\chi$  deviates slightly from the assumed value of unity in the calculations below, the resulting free energy of activation will be too high. However, the error should be common to all the halogenated ethanes considered, so that the barriers can be quantitatively compared.

In Eq. (15) one must use the difference in free energies between the potential minimum and the potential barrier. However, energies of activation would be more satisfactory quantities to correlate between molecules. It seems reasonable to assume that only small changes result in all of the vibrational frequencies of a molecule as internal rotation occurs, except for the torsional mode which has zero frequency at the top of the barrier and a sizeable frequency in any of the minima. This

latter mode is, hence, the only mode to contribute substantially to  $\Delta S^\ddagger$ , the entropy of activation. Calculations show that  $T\Delta S^\ddagger$  resulting from this last vibration for any of these halogenated ethanes at the temperature under consideration is approximately 0.5 kcal/mole, and does not vary by more than  $\pm 0.2$  kcal/mole from one molecule to another. This variation is of the same order of magnitude as our experimental error. Since exact corrections cannot be made, this variation will be ignored.

Hence, for all molecules under consideration, the energies of activation are approximately 0.5 kcal/mole less than the free energies of activation. Since this is a constant term, it is of little importance in the correlation of barriers with molecular structure. It will henceforth be ignored. All numbers appearing in the remainder of the text which are referred to as energies of activation are in fact free energies of activation.

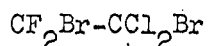
#### Experimental

$\text{CFCl}_2\text{-CFCl}_2$  was obtained from K & K Laboratories and  $\text{CF}_2\text{Br-CFCl}_2\text{Br}$  from Peninsular Chemresearch Inc.  $\text{CF}_2\text{Br-CFBr}_2$  and  $\text{CF}_2\text{Br-CHBrCl}$  were prepared by bromination of  $\text{CF}_2=\text{CFBr}$  (Peninsular Chemresearch Inc.) and  $\text{CF}_2=\text{CHCl}$  (Allied Chemical Corp.) in the same manner as  $\text{CF}_2\text{Br-CFBrCl}$  has been prepared.<sup>20</sup>

The spectra were recorded on a Varian HR-60 spectrometer operating at 56.4 Mc/sec equipped with a flux stabilizer and integrator. Chemical shifts and coupling constants were determined by the usual audio sideband technique, when the resonance lines were sharp. At intermediate rates of exchange the lines were broad and two sidebands of the fluorinated

solvent were used, one on each side of the peaks of interest. Most of the spectra were obtained at fairly rapid sweep rates (about 200 cps/minute), using short response times, in order to avoid saturating the broad peaks at reasonable power levels. All frequency differences and line widths tabulated in the tables are the average of at least 8 spectra. The experimental errors are the root-mean-square deviations. The separations between the peaks and line widths were measured to  $\frac{1}{2}$  or 1 cps from the computer spectra, depending on the width of the peak. The computer results for  $\text{CF}_2\text{Br}-\text{CCl}_2\text{Br}$  were obtained more accurately below  $220^\circ\text{C}$  by interpolation from the printed absorbances in order to observe small differences in the widths.

The variable temperature insert has been described previously.<sup>6</sup> Although the absolute temperature is only known to  $\pm 2$  or  $3^\circ$ , the differences in temperature for spectra taken on a given run are known more accurately.



The variable temperature spectra of  $\text{CF}_2\text{Br}-\text{CCl}_2\text{Br}$  were taken in a 25% mole fraction solution in  $\text{CFCl}_3$ . The low temperature spectrum at  $191^\circ\text{K}$ , shown in Fig. 2, consists of a large peak (labelled peak 1 in Table I and the discussion below) about 3313 cps upfield from the solvent and an AB quartet of peaks centered 205.9 cps upfield from peak 1. From the schematic diagram of the three rotamers of  $\text{CF}_2\text{Br}-\text{CCl}_2\text{Br}$  in Fig. 3, it is seen that rotamer I has a plane of symmetry which makes the two fluorines equivalent. Rotamers II and III are mirror images which differ by the interchange of their two fluorines. Consequently rotation between II and III does affect the spectrum. Peak 1 is unambiguously assigned

to rotamer I and the quartet to the pair of rotamers II and III. The chemical shift,  $\nu_A - \nu_B$ , and the coupling constant,  $J_{AB}$ , of the two fluorines on II or III are  $184.8 \pm .6$  and  $155.8 \pm .6$  cps, respectively.

The ratio of the areas of peaks 3 and 4 relative to 1 and 2 was measured with the Varian integrator. From the known coupling constants and chemical shifts of the AB quartet, the area of peak 2 was calculated and used to find the area of peak 1 alone. This calculation indicated that the relative populations of I: (II + III) =  $1.16 \pm .06$ : 1.00. Hence rotamers II and III are  $320 \pm 20$  cal/mole higher in energy than rotamer I.

As the temperature is increased the peaks broaden. At  $198^\circ\text{K}$  peak 2 is unobservable due to the 5 cps width of the much larger peak 1. Above  $206^\circ$  peak 5 is not distinguishable from the noise. However, the coalescence of the remaining three peaks, 1, 3, and 4, was carefully studied. Initially it was attempted to fit the spectra assuming that the transmission coefficient was much less than one. As will be shown later choosing all three barriers the same, or the barrier between rotamers II and III less than the other two barriers, gives calculated spectra which show peaks 3 and 4 coalescing prior to the coalescence of peaks 1 and 3. As is pointed out below, this is not observed. It is necessary to assume that interconversion of rotamers II and III (barrier  $E_5$ ) is slower than the exchange between I and II ( $E_4$ ) or I and III ( $E_6$ ) to reproduce the experimental spectra.  $E_4$  and  $E_6$  are equal by symmetry.

All spectra were calculated using Eq. (15). This equation is always correct for  $\kappa = 1$  and is valid for  $\kappa < 1$  if  $E_5$  is set equal to  $E_4$  and  $E_6$ . In this latter case, the resultant calculated barriers are low by a

constant factor,  $-RT \ln \kappa$ . For  $E_5 < E_4$ , and  $\kappa < 1$ , a new set of equations must be used.<sup>6</sup>

Before describing the spectra, we consider the temperature dependence of the intermolecular interaction with the solvent on the chemical shifts. The two fluorines are on the same carbon atom and previous work on  $\text{CF}_2\text{Br-CFBrCl}$ <sup>20</sup> shows that they should be nearly equally affected by the intermolecular interaction. The effect on the two different rotamers should also be similar. These conclusions are confirmed by observing that the chemical shift between peaks 3 and 4 is constant from 191°K to 224°, when the peaks begin to coalesce. The chemical shift between peaks 1 and 3 is constant from 191° to 210°. There remains a significant temperature dependence of the chemical shifts from the solvent. The frequency of the observed, symmetrical, singlet peak at 257°K is 2300.1 cps upfield from the solvent. From the chemical shifts measured at 198° and the time average approximation, the frequency of the peak at 257° is calculated to be 2318.0 cps and is independent of small changes in the barriers. It is also clear from the  $2\frac{1}{2}$  cps downfield shift of peak 1 between 198° and 206° that there is a temperature-dependent shift of the solute peaks from the solvent, since coalescence of the solute peaks would cause an upfield shift. In order to compare the observed shifts of peak 1 (and, at higher temperature, the large single peak) with the calculated ones, it is easiest to correct the observed shifts for this solvent affect. Assuming a linear function between 198° and 257°, the corrected chemical shifts tabulated in Table I are given by

$$\nu'_{\text{obs}} = \nu_{\text{obs}} - 0.305 (T - 198), \quad (18)$$

Table I

Calculated and observed frequency separations and line widths for  $\text{CF}_2\text{Br}-\text{CCl}_2\text{Br}$  in  $\text{CFCl}_3$ .<sup>a</sup> Peaks are numbered as in Fig. 2. The experimental spectra are shown in Fig. 4, and some of the calculated spectra at  $222\frac{1}{2}^\circ\text{K}$  have been reproduced in Fig. 5. All values are in cps, at 56.4 Mc/sec.

Temp.	$E_4^b$	$E_5^b$	$\nu_{\text{obs}}^c$	$\nu_1 - \nu_3$	$\nu_3 - \nu_4$	$W_1^{\frac{1}{2}d}$	$W_3^{\frac{1}{2}d}$	$W_4^{\frac{1}{2}d}$
198°K	Exp.		0.0 ±.4	162.3 ±.4	86.3 ±.4	5.0 ±.2	4.9 ±.2	4.9 ±.2
	10.8	12.0	0	$162\frac{1}{2}$	86	5.4	5.7	5.6
	10.85	10.85	0	$162\frac{1}{2}$	86	4.9	6.2	6.2
	10.85	11.6	0	$162\frac{1}{2}$	86	4.9	5.3	5.3
	10.85	12.0	0	$162\frac{1}{2}$	86	4.9	5.2	5.2
	10.85	13.0	0	$162\frac{1}{2}$	86	4.9	5.2	5.2
	10.9	12.0	0	$162\frac{1}{2}$	86	4.6	4.9	4.8
206	Exp.		-0.2 ±.3	162.9 ±1.4	87.0 ±.8	12.2 ±.5	13.7 ±.6	13.6 ±.9
	10.75	12.0	1	161	86	13.1	15.3	15.0
	10.8	10.8	$\frac{1}{2}$	$161\frac{1}{2}$	86	12.5	17.5	17.3
	10.8	11.6	1	161	86	12.1	14.1	13.9
	10.8	12.0	1	161	86	12.1	13.9	13.8
	10.8	13.0	1	161	86	12.1	13.7	13.5
	10.85	13.0	1	161	86	11.4	12.5	12.4
216 $\frac{1}{2}$	Exp.		2.1 ±.6	156.6 ±1.5	87.2 ±1.5	30.2 ±1.2	33.7 ±2.0	33.8 ±2.0
	10.75	13.0	3	154	87	$31\frac{1}{2}$	40.	$40\frac{1}{2}$
	10.8	12.0	3	$154\frac{1}{2}$	87	$29\frac{1}{2}$	37.	$37\frac{1}{2}$
	10.8	13.0	$3\frac{1}{2}$	$154\frac{1}{2}$	87	$28\frac{1}{2}$	$36\frac{1}{2}$	37
	10.85	10.85	3	157	84	$32\frac{1}{2}$	$43\frac{1}{2}$	46
	10.85	11.6	3	156	87	$28\frac{1}{2}$	$37\frac{1}{2}$	38
	10.85	12.0	3	156	86	$27\frac{1}{2}$	34	34
	10.85	13.0	3	156	86	$26\frac{1}{2}$	$33\frac{1}{2}$	$33\frac{1}{2}$
	10.9	10.9	3	157	84	28	$41\frac{1}{2}$	$45\frac{1}{2}$
	10.9	11.3	$2\frac{1}{2}$	$156\frac{1}{2}$	87	$27\frac{1}{2}$	34	$34\frac{1}{2}$

Table I continued

Temp.	$E_4^b$	$E_5^b$	$v_{obs}^c$	$v_1 - v_3$	$v_3 - v_4$	$w^{3/4^d}$	$w^{2/3^d}$
222½°	Exp.		14.5 ±1.2	122. ±7.	83. ±7.	49.3 ±2.5	61.6 ±2.5
	10.7	11.6	16	112	84	51	63½
	10.7	12.0	15	115	90	48½	62½
	10.75	10.75	17	121	e	52½	65½
	10.75	11.2	15	123	82	48	59½
	10.75	11.6	13	126	88	43½	54½
	10.75	12.0	12	126	92	41½	51
	10.8	10.8	14	134	e	45½	56
230°	Exp.		76 ±8.			93. ±4.	111. ±4.
	10.75	10.75	78			88	106
	10.75	11.2	75			85	102½
	10.75	11.6	75			86	103
	10.75	12.0	76			87	105
	10.8	10.8	71			98½	117½
	10.8	11.2	68			94½	114
	10.8	11.6	69			97	116
	10.8	12.0	69			101	118½
	10.85	11.2	58			103	123

Temp.	$E_4^b$	$E_5^b$	$v_{obs}^c$	$w^{1/2^d}$
247°	Exp.		100.3 ±2.1	48.1 ±2.3
	10.8	12.0	101	44
	10.85	11.4	102	44
	10.85	12.0	101	48
	10.85	13.0	100	49½
	10.9	10.9	103	41½
	10.9	11.4	101½	47½
	10.9	12.0	100	51½
	11.0	11.0	102½	51

Table I continued

- 
- a Spectra were calculated using Eqs. (8-13) and (15). The observed chemical shift from  $\text{CFCl}_3$  and the width of a sideband of the solvent peak, taken as the natural line width in the calculation, were 3112.6 and 2.0 at  $198^\circ$ , 3110.0 and 3.0 ( $206^\circ$ ), 3109.1 and 2.7 ( $216\frac{1}{2}^\circ$ ), 3119.6 and 2.9 ( $222\frac{1}{2}^\circ$ ), 3179.0 and 3.0 ( $230^\circ$ ), and 3198.0 and 5.0 ( $247^\circ$ ).
- b  $E_4 = E_6$ , and  $E_5$  in kcal/mole.
- c  $\nu_{\text{obs}}$  is the chemical shift corrected according to equation 18 and less 3112.6 cps.
- d  $W^{3/4}$  is the width of the main peak at  $3/4$  height, etc. At  $216\frac{1}{2}^\circ$  the width is obtained from the dashed line shown in Fig. 4.
- e Coalesced.
-



where T is the absolute temperature. The experimental chemical shifts from the solvent are listed in footnote a of Table I.

The experimental spectra are shown in Fig. 4 at several temperatures. The chemical shifts and line widths are tabulated in Table I for the experimental and several calculated spectra.

At 198°K the spectrum calculated with  $E_4 = 10.85$  kcal/mole reproduces the observed width of peak 1. The spectra calculated with all three barriers the same makes peaks 3 and 4 broader than peak 1 because the chemical shift between the fluorines which are exchanging when II rotates to III is less than the average chemical shift between the fluorines on I and II or III. Increasing  $E_5$  prevents direct interconversion of II and III;  $E_5 \geq 12.0$  kcal/mole gives the proper width of peaks 3 and 4. The experimental spectrum at 206° is similar to the one at 198°; it is reproduced with  $E_4 = 10.8$  and  $E_5 \geq 12.0$ .

At 216½°K there is a set of values of  $E_4$  and  $E_5$  which reproduce fairly well the observed spectra. Three members of this set are 10.8 and 13.0, 10.85 and 12.0, or 10.9 and 11.3. If  $E_4 = E_5$  then the difference in widths of peaks 1 and 3 is much larger than observed. The half-widths have been measured from the dashed line in the spectra, which introduces an added uncertainty of choosing the proper base line. It is impossible to measure the half width of peaks 3 and 4 from the true base line due to overlap with peak 1.

Several calculated spectra at 222½°K are shown in Fig. 5. The calculated spectra with  $E_5 \leq E_4$  clearly show peaks 3 and 4 coalescing before peaks 1 and 3 coalesce, whereas the experimental spectrum shows both 3 and 4 as discernible peaks on the side of peak 1.  $E_4 = 10.7$ ,

$E_5 = 12.0$  and  $E_4 = 10.75$ ,  $E_5 = 11.2$  both duplicate the experimental spectrum. If the barriers are the same, then peak 3 cannot be seen while maintaining the observed chemical shift between peaks 1 and 2 in the calculated spectra.

At  $230^\circ\text{K}$  the set of barriers which reproduce the observed spectrum includes  $E_4 = 10.8$ ,  $E_5 = 11.2$  and  $E_4 = 10.85$ ,  $E_5 = 12.0$ . Choosing all barriers equal reproduces the observed line width and frequency at this relatively high temperature only because of the symmetrical appearance of the spectrum.  $E_4 = E_5 = 10.8$  has approximately the same width as  $E_4 = 10.8$  and  $E_5 = 12.0$ , but the former is a more symmetrical peak whereas the latter has a much larger upfield tail. At high values of  $E_5$  an upfield peak (due to rotamers II and III) of sufficient intensity to cause a slight increase in the widths is being superimposed on the main peak.

At  $247^\circ\text{K}$  there is a set of barriers which will fit the observed spectrum. At this relatively high temperature the lines are narrower and the effects of  $E_5$  on the spectra are readily noticed. If the barriers were the same it would be necessary to increase  $E_4$  to 11.0 to reproduce the spectrum, whereas  $E_4 = 10.85$  and  $E_5 = 12.0$  provides an equally good fit.

The above data show that choosing the barriers in  $\text{CF}_2\text{Br}-\text{CCl}_2\text{Br}$  as  $E_4 = E_6 = 10.8 \pm .1$  kcal/mole and  $E_5 \geq 12.0 \pm .5$  kcal/mole can reproduce the experimental spectra over the 60 degree temperature range in which the coalescence of the peaks can be observed. Spectra have been taken at several additional temperatures with results substantially similar to those described above. These spectra as well as several additional calculated spectra are depicted elsewhere.<sup>14</sup>

Qualitative results were also obtained in  $\text{CS}_2$  solution. In this solvent the lower barrier was the same, or possibly slightly lower, than in the  $\text{CFCl}_3$  solution. Since the absence of a solvent fluorine resonance made it impossible to estimate the field homogeneity quantitative comparisons were impossible.

$\text{CFClBr-CFClBr}$

Thompson, Newmark, and Sederholm<sup>6</sup> obtained the barriers in  $\text{CFClBr-CFClBr}$  using the Bloch-McConnell equations. Since the density matrix theory can reproduce the observed doublets due to spin-spin splitting, the spectra have been recalculated. There are two isomers, each consisting of three rotamers, which are drawn in Fig. 6. The spectrum at  $177^\circ$  is shown in Fig. 7. The second and third rotamers of the first isomer are mirror images and have identical AX spectra. The fluorines in all the other rotamers are equivalent and only one line is observed for each rotamer.

The analysis of the low temperature spectra has been described in detail by Thompson et. al.<sup>6</sup> Based on their assignment, IIa resonates at peak e in Fig. 7, IIb at peak a, and IIc at peak h.  $E_4'$  is the barrier between rotamers IIa and IIb,  $E_5'$  between IIa and IIc, and  $E_6'$  between IIb and IIc. Note that IIb has the bromines trans and is assumed to be the stable configuration. Primes have been used to distinguish the barriers in isomer II from those in isomer I. The assignment for rotamer I is unambiguous since Ib and Ic contribute equally to the doublet peaks b, c, f, and g. The remaining peak, d, is assigned to Ia.  $E_4$  is the barrier between Ia and Ib, and is equal by symmetry to  $E_6$ , the barrier between Ia and Ic.  $E_5$  is the barrier between the mirror image rotamers, Ib and Ic.

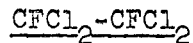
The exchange between the rotamers of the second isomer can be described exactly by the modified Bloch equations since no coupling is observable. The spectra at intermediate rates of exchange have only been obtained in  $\text{CS}_2$ . Since the field homogeneity is not known, only qualitative results are reported here. There are two main differences between the barriers reported here and those determined previously. First, kinetics based on  $\kappa = 1$  have been used, so that all the barriers are about .4 kcal./mole higher than previously reported. Second, it is possible to observe the two different barriers in the first isomer by observing the coalescence of the doublets due to rotamers Ib and Ic.

The experimental spectrum and several calculated spectra at  $194^\circ\text{K}$ . are shown in Fig. 8. A natural line width of 3.0 cps has been assumed for the calculations. This is reasonable since the spectra were taken after obtaining a good field at a temperature only  $10^\circ$  lower where the lines are sharp. The observed ratio of the heights of peaks a and h requires that  $E_5^i$  and  $E_6^i$  (denoted as EP5 and EP6 on the computer output) be about .8 kcal/mole greater than  $E_4^i$ . Choosing either  $E_5^i$  much larger, about 1 kcal./mole, than  $E_6^i$ , or  $E_6^i$  much larger than  $E_5^i$  makes peak h much sharper than peak a. This effect occurs since either condition restricts the rotation of species IIc (peak h) significantly more than it affects IIa (peak a). IIa is already undergoing rapid exchange with IIb and its resonance becomes essentially independent of  $E_5^i$  after  $E_5^i$  becomes about .5 kcal./mole greater than  $E_4^i$ . A small difference between  $E_5^i$  and  $E_6^i$  is not detectable within the present experimental error, so the two barriers were set equal for the remainder of the calculations. The best width for peaks a and h is then obtained with  $E_4^i = 9.8$  kcal./mole

and  $E_5' = 10.5$  kcal./mole. Using these values, the observed width of peaks d and e is obtained with  $E_4 = 10.1$  kcal./mole. Finally, the doublets are only observed if  $E_5$  is increased substantially above  $E_4$ , to 11.0 or 12.0. Although the doublets could be observed by making  $E_4$  and  $E_5$  the same, about 10.4, the width of peaks d and e is much too sharp. This confirms the conclusions reached in the analysis of the  $\text{CF}_2\text{Br}-\text{CCl}_2\text{Br}$  data that the highest barrier is necessary to reproduce the observed spectra, and consequently the transmission coefficient must be near unity.

Experimental spectra have also been taken at  $207^\circ$  and  $233^\circ\text{K}$ .<sup>6</sup> At  $207^\circ\text{C}$  the experimental spectrum is duplicated with  $E_4' = 9.9$ ,  $E_5' = 10.8$ ,  $E_4' = 10.2$ , and  $E_5' = 12.0$  at a line width of 3.0 cps. That it is necessary to increase all the barriers by approximately equal amounts probably indicates a small error in the temperature measurement. At  $233^\circ\text{K}$  it is possible to reproduce the experimental spectrum with the same choice of barriers which gave the best fit at  $194^\circ\text{K}$  if a natural line width of 20 cps is used.<sup>14</sup> The magnet inhomogeneity may have been this large for these spectra, and cannot be determined in the nonfluorinated solvent.

The reinvestigation of the data for this compound show that the barriers are unchanged with temperature, within experimental error, and are given approximately by the values determined at  $194^\circ\text{K}$ .



A third compound containing only two fluorines has also been studied. There are two identical rotamers of  $\text{CFCl}_2-\text{CFCl}_2$  with the fluorines gauche to each other. The third rotamer has the fluorines trans. In both rotamers the fluorines are equivalent. A 33% by volume solution in  $\text{CFCl}_3$

was prepared. The compound was contaminated by about 25%  $\text{CF}_2\text{Cl}-\text{CCl}_3$ . The single resonant peak of the latter occurs 65.086 ppm upfield from  $\text{CFCl}_3$ , and  $2.722 \pm .006$  ppm downfield from the single  $\text{CFCl}_2-\text{CFCl}_2$  peak at room temperature. This impurity peak did not interfere with the interpretation at any temperatures. Tiers<sup>21</sup> has obtained a shift of  $2.755 \pm .01$  ppm at  $21^\circ\text{C}$  for a 90% solution of the difluoroethanes in  $\text{CFCl}_3$ ; the difference from our value is due to the chemical shift dependence on the temperature and solvent concentration.

At low temperatures exchange is sufficiently slow that the spectrum due to  $\text{CFCl}_2-\text{CFCl}_2$  consists of two sharp lines, with relative areas of 1.00:  $1.33 \pm .03$  at  $151^\circ\text{K}$ . Assuming the trans rotamer is the lowfield peak, then the degenerate gauche rotamers comprise the highfield peak, and the energy of the gauche forms is  $122 \pm 7$  cal/mole above the trans form.

The chemical shifts,  $\nu_1$  and  $\nu_2$ , of the rotamers from the solvent are tabulated in Table II. These have been plotted against temperature at low temperatures where exchange does not affect the transition frequencies. Extending the straight lines to  $300^\circ\text{K}$  gives chemical shifts of 3767. cps and 3866. cps, respectively. Using the "time average" approximation,<sup>20</sup> the chemical shift at  $300^\circ$  is calculated to be 3828. cps, which compares well with the experimental value of 3824. cps considering the narrow temperature range over which the chemical shift of the individual rotamers has been obtained.

The alternative assignment of the low temperature spectrum, choosing the trans rotamer as the highfield peak, yields gauche rotamer energies of 294 kcal/mole. Then the spectrum observed at  $194^\circ\text{K}$  should consist of two peaks of equal intensity, contrary to experiment. Further, the chemical shift at room temperature calculated from the "time average" approximation would be 3811. cps.

Table II.

Chemical shifts, peak widths, and barrier to rotation of  $\text{CFCl}_2$ -  
 $\text{CFCl}_2$  in  $\text{CFCl}_3$ . All frequencies are in cycles per second at  
 56.4 Mc. Experimental spectra are shown in Fig. 9.

Temp.	Doublet Separation	a $\nu_1$	a $\nu_2$
151°K	57.91 ± .25	3839.7 ± .5	3897.6 ± .5
154	58.9 ± .3	3837.4 ± .3	3896.3 ± .3
160	59.6 ± .3	3835.6 ± .5	3895.2 ± .5
167	61.9 ± .3	3831.6 ± .3	3893.5 ± .3

Temp.	b $2/T_2$	Doublet Separation	Width <sup>c</sup> Peak 1	Width <sup>c</sup> Peak 2	d Barrier
177°K	2.6 ± .3	63.1 ± .5	6.8 ± .3	6.0 ± .3	9.5
186 $\frac{1}{2}$	4.4 ± .3	62.6 ± .6	16.3 ± .6	13.0 ± .4	9.7
188	3.2 ± .3	62.4 ± 1.1	17.7 ± 1.0	13.1 ± 1.0	9.7
191	7.0 ± 1.0	52.8 ± 3.	—	28. ± 4.	9.6
194	4.6 ± .7	45. ± 2.	—	30. ± 4.	9.65
196 $\frac{1}{2}$	6.4 ± 1.0		(2.0)	61. ± 3.	9.6
198	2.8 ± .3		(1.5)	50. ± 3.	9.6
200	2.8 ± .4		(1.1)	38. ± 2.	9.6
204	2.6 ± .5			24. ± 2.	9.6
213	4.8 ± 1.0			12.8 ± .6	9.6

a Chemical shifts from the solvent,  $\text{CFCl}_3$ .

b Width at half height of solvent sideband.

c Width at half height. Above 190°K there is only one peak; its width is given in the peak 2 column. The numbers in parentheses in the peak 1 column denote the asymmetry of this peak, calculated as the ratio of the distance, at half height, from the center of the peak to the low field

Table II continued

side divided by the distance from the center to the high field side, where the center is that point under the maximum of the peak.

- d The barrier is obtained by comparison to the calculated spectra. The parameters obtained from these spectra are tabulated for several values of the barrier at each temperature in Table IV of reference 14.
- 
-



There is also a linear dependence of the chemical shift between rotamers with temperature of 0.20 cps/degree. It was assumed that the temperature dependence remained linear at all temperatures and spectra were calculated using a corrected chemical shift,

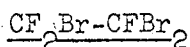
$$\nu_T = \nu_{150} + 0.20 (T - 150) \quad (19)$$

where  $\nu_T$  is the chemical shift at temperature T.

The experimental spectra at several temperatures are shown in Fig. 9, and the line widths and chemical shifts are tabulated in Table II. Since exchange between the two gauche rotamers does not change the environment of the fluorine atoms, this rate is unobservable. The only observable barrier is for the rotation between the trans form and either one of the gauche forms. The spectra were calculated with the Bloch-McConnell equations since no spin-spin coupling is observable in the rotamers. Since only two species are observed, identical results can be obtained using the expression developed by Gutowsky and Holm,<sup>22</sup> but with an additional factor of two in the rate to account for the two possible paths of rotation.

The calculated spectra appear identical to the observed spectra in Fig. 9 for the proper exchange rate. The inhomogeneity of the magnetic field, obtained from the width of the solvent sidebands used to calibrate the spectrum, contributed significantly to the width of the peak at some temperatures and were included in the calculation.

The barrier was obtained at each temperature by comparison of the calculated and experimental spectra, and the best value at each temperature is also listed in Table II. The mean value of the barrier is  $9.6 \pm .1$  kcal/mole, independent of temperature.



The low temperature spectrum of the three rotamers of CF<sub>2</sub>Br-CFBr<sub>2</sub> in carbon disulfide was first observed by Manatt and Elleman.<sup>23</sup> Spectra were first taken in CS<sub>2</sub>, but the sample always froze before the low intensity peaks of the spectrum, broadened by exchange, could be observed. It is also convenient to use a fluorinated solvent in order to improve the field homogeneity conveniently at low temperatures. Therefore, the barriers were obtained in a solution 40% by volume in CF<sub>2</sub>Cl<sub>2</sub>.

The three rotamers are drawn in Fig. 10, and the spectrum at 152°K is shown in Fig. 11. Rotamers I and II have identical ABX spectra, and peaks 1-8 and 11-13 are clearly attributed to this rotamer. The remaining five peaks comprise an A<sub>2</sub>X spectrum due to rotamer III, in which two of the fluorines are equivalent. The additional peaks between peaks 8 and 9 in Fig. 10 are due to impurities; these peaks remained sharp at all temperatures. At 145°K, peaks 1, 2, 7, and 8 are as sharp as peaks 3-6, but it is then impossible to observe the triplet of rotamer III, as the population of this rotamer decreases rapidly with temperature. However, the coupling constants and chemical shifts (in cps from the solvent) of rotamer I could be accurately determined —  $J_{AB} = 168.1$ ,  $J_{AX} = -16.1$ ,  $J_{BX} = -18.4$ ,  $\nu_A = 2843.5$ ,  $\nu_B = 3014.2$ , and  $\nu_X = 3616.9$  cps.

At 146°K the relative areas of peaks 7-8 and 9-10 is  $1:2.023 \pm .14$ , from which the energy of rotamer III (relative to rotamer I) is 760 kcal/mole. The coupling constant and chemical shifts for the third rotamer were obtained at 150°K —  $J_{AX} = -21.5$ ,  $\nu_A = 3330.5$ , and  $\nu_X = 3885.2$  cps. The signs of the coupling constants were determined as follows. Manatt and Elleman<sup>23</sup> showed that  $J_{AX}$  and  $J_{BX}$  in rotamer I are negative,

assuming  $J_{AB}$  is positive. Presuming that time averaging is qualitatively valid, the coupling constant at room temperature is calculated with both positive and negative signs for  $J_{AX}$  in rotamer III. The results are -15.3 and -17.6. The experimental value in  $CS_2$  is  $|17.1|$ , from which it follows that  $J_{AX}$  in rotamer III is also negative.

As the temperature is increased above 150°K peaks 1-2 and 7-8 of the AB octet become significantly broader than peaks 3-6 (Fig. 11). As the temperature is increased further the outer peaks can no longer be distinguished from the noise, and only the central AB quartet was studied. This region is shown at four higher temperatures in Fig. 12. At 163° the quartet is collapsing into two peaks. The entire spectrum at 167° is shown in Fig. 13. All of the peaks are sharp except those due to the AB octet of rotamers I and II. The latter coalesces to a broad line about 90 cps wide at 171°. As the temperature is increased further this sharpens into a doublet, observed at 185°. At higher temperatures the doublet coalesces and the triplet (peaks 11-13), which remains sharp until 185°, broadens and coalesces at about 197°K. Several spectra of the triplet peaks are shown in Fig. 12. Above 213° the triplet reappears, and the doublet forms again above 217°. At room temperature an  $A_2X$  spectrum consisting of five sharp lines is observed.

The results are qualitatively explained for exchange between three ABX systems by the following argument.  $E_4$ , the barrier between rotamers I and II, is much less than  $E_5$ , the barrier between rotamers II and III. By symmetry,  $E_6$ , the barrier between I and III, is equal to  $E_5$ . Rotation from I to II occurs at relatively low temperatures, which interchanges the position of the A and B fluorines, but doesn't change the environment

of the X nucleus. The X region of the spectrum and the doublet of rotamer III are only affected by rotation from I or II to III. This does not occur to an appreciable extent until you reach the high temperature end of the coalescence range. Thus the triplets remain sharp until about 185°K. The doublet in the AB region is observed from 185° to about 197° since the exchange between I and II has become so fast that the fluorines are almost averaged. Above 200°,  $E_{11}$  has only a minor effect on the AB part of the spectrum. The X portion is independent of  $E_{11}$  at all temperatures.

The frequency separations and peak widths for the observed and calculated spectra at several temperatures are tabulated in Table III for the AB region and Table IV for the X peaks. The calculated spectra reproduce the appearance of the experimental spectra for the proper choice of the barriers and are not shown here. Qualitatively, the chemical shifts tabulated in Table III are explained as follows. There is a downfield shift of the AB octet with temperature, due to intermolecular interactions with the solvent, until about 185°K. At this point the octet begins to coalesce with the much less intense doublet of rotamer III, and only an averaged  $A_2$  spectrum is observed of all three rotamers at a weighted intermediate frequency. As the temperature rises the population of rotamer III increases, which would shift the lines upfield. However the downfield chemical shift of the individual rotamers with temperature causes an approximately equal and opposite effect, so that the frequency of the doublet is essentially unchanged from 219° to 237°.

The center of the AB region at 237° is observed 2937.6 cps upfield from the solvent, whereas the chemical shift is calculated to be 2965.0 cps from the low temperature data, a discrepancy of 30.4 cps. At 185°

Table III

Calculated and observed frequency separations and line widths for the AB region of  $\text{CF}_2\text{Br}-\text{CFBr}_2$  in  $\text{CF}_2\text{Cl}_2$ .<sup>a</sup> Peaks are numbered as in Fig. 11 at low temperatures. The doublet observed at temperatures above 167°K is labelled as peaks 4 and 5.  $w_{4,5}$  is the width, at half height, of peaks 4 and 5 together. The experimental spectra are shown in Figs. 12-13. The calculated spectrum with an asterisk give the best fit to the experimental spectrum. All values are in cps.

Temp.	$E_4^b$	$E_5^b$	$\nu_3-\nu_4$	$\nu_4-\nu_5$	$\nu_5-\nu_6$	$w_{3,4}$	$w_{5,6}$
163°K		Exp.	11.1	47.9	14.7	38.5	39.6
			$\pm 1.0$	$\pm 0.6$	$\pm 0.6$	$\pm 2.0$	$\pm 2.0$
	7.6	9.9	12	$51\frac{1}{2}$	$14\frac{1}{2}$	$41\frac{1}{2}$	$43\frac{1}{2}$
	7.65	9.9*	$13\frac{1}{2}$	$52\frac{1}{2}$	$15\frac{1}{2}$	38	$39\frac{1}{2}$
	7.7	9.9	14	53	16	$35\frac{1}{2}$	36
Temp.	$E_4^b$	$E_5^b$	$\nu_4-\nu_5$	$w_{4,5}$			
167°K		Exp.	$54 \pm 2$	$95 \pm 2$			
	7.6	9.9	47	$95\frac{1}{2}$			
	7.7	9.9*	57	$102\frac{1}{2}$			
174		Exp.	c	$68 \pm 2\frac{1}{2}$			
	7.6	9.7	c	58			
	7.6	9.9*	c	58			
	7.7	9.9	c	73			
	7.6	10.1	c	58			

Table III continued

Temp.	$E_4^b$	$E_5^b$	$\nu_4 - \nu_5$	$w_{4,5}$	$\nu_{AB}^d$
185°		Exp.	$9 \pm 2$	$42 \pm 1$	$2907.7 \pm 1$
	7.7	9.9	14	$36\frac{1}{2}$	2929
	7.8	9.8	9	41	2929
	7.8	9.9*	9	40	2929
	7.8	10.0	10	$39\frac{1}{2}$	2929
	7.9	9.9	c	44	2929
	7.9	10.0	c	$43\frac{1}{2}$	2929
210		Exp.	c	$49.0 \pm 1.5$	$2924.5 \pm 1.2$
	7.7	9.8	c	$45\frac{1}{2}$	2951
	7.7	9.9*	c	47	$2947\frac{1}{2}$
	7.7	10.0	c	47	$2943\frac{1}{2}$
	7.7	10.1	c	$45\frac{1}{2}$	2940
	7.9	9.9	c	47	$2947\frac{1}{2}$
237		Exp.	$16.7 \pm .9$	$9.5 \pm .7$	$2937.6 \pm .3$
	7.7	10.0	$17\frac{1}{2}$	7.7	2965
	7.7	10.1*	$17\frac{1}{2}$	9.6	2965

- a Spectra were calculated using Eqs. (8-13) in the ABX approximation and Eq. (15). The natural line width, in the absence of exchange, used in the calculations was 2.6 (163°K), 3.2 (167°), 2.5 (174°, 185°), 2.3 (210°), and 1.8 (237°).
- b  $E_4, E_5 = E_6$  in kcal/mole.
- c Lines coalesced.
- d  $\nu_{AB}$  is the chemical shift of the AB line (s) from the solvent. Below 185°K the calculated values are all 2929 cps, the experimental values are

Table III continued

2918.6 (163°), 2916.0 (168°), and 2908.1 (174°). The chemical shifts corrected for the temperature dependent intermolecular solvent interaction (see text) are 2929 (185°), 2950 (210°), and 2965 (237°).

---

---

the discrepancy between the observed and calculated value for the location of the AB octet is 21.5 cps, and at 152° the difference is about zero. Either a nonlinear temperature dependence or a substantially different temperature dependence for the chemical shifts of the two different rotamers appears necessary to explain these three points. Nevertheless, assuming the difference is linear between 185° and 237°, then the corrected values of the chemical shifts are within experimental error of the calculated values (see footnote d. of Table III).

The data in Tables III and IV indicate the best values for the barriers to internal rotation are  $E_4 = 7.7 \pm .2$  kcal/mole and  $E_5 = E_6 = 9.9 \pm .2$  kcal/mole. Although the experimental spectrum at any temperature can be reproduced, the best value for the barrier  $E_4$  varies randomly from 7.6 to 7.9, and for  $E_5$  from 9.7 to 10.1, due to the error in determining the temperature in these experiments. At most temperatures changing the barrier by .1 kcal/mole changes the appearance of the calculated spectrum sufficiently that the best value is readily determined. This is quantitatively seen from the widths of the peaks given in Tables III and IV.

CF<sub>2</sub>Br-CFBrCl

Brey and Ramey<sup>24</sup> first obtained the low temperature spectrum of the three rotamers of this compound. The assignment of the low temperature spectrum is discussed in detail by Newmark and Sederholm.<sup>20</sup> In the spectrum at 150°K (Fig. 14) peaks 1-6, 10-11, and 16-18 are assigned to an ABX spectrum of rotamer I; peaks 9, 12-15, and 22-24 to rotamer III, and peaks 7-8 and 19-21 to rotamer II. The fluorines in II are nearly degenerate. The chemical shift between the fluorines in rotamer II was



Table IV

Calculated and observed frequency separations and line widths for the X region of  $\text{CF}_2\text{Br-CFBr}_2$  in  $\text{CF}_2\text{Cl}_2$ .<sup>a</sup> Only the triplet, peaks 11-13 in Fig. 11, was studied.  $w^{\frac{1}{4}}$  is the width at  $\frac{1}{4}$  height of peak 12, and  $w^{\frac{1}{2}}$  is the width at  $\frac{1}{2}$  height. The latter, as seen from the spectra reproduced in Fig. 12, usually includes part of peaks 11 and 13. The calculated spectra with an asterisk give the best fit to the experimental spectra.

Temp.	$E_5^b$	$\nu_{11}-\nu_{12}$	$\nu_{12}-\nu_{13}$	$w^{\frac{1}{4}}$	$w^{\frac{1}{2}}$
188°K	Exp.	$17.0 \pm .4$	$16.8 \pm .5$	-	$8.7 \pm .6$
	9.7*	17	$17\frac{1}{2}$		$9\frac{1}{2}$
	9.8	$17\frac{1}{2}$	$17\frac{1}{2}$		$7\frac{1}{2}$
	9.9	$17\frac{1}{2}$	$17\frac{1}{2}$		$6\frac{1}{2}$
196	Exp.	$14.5 \pm 1.0$	$15.7 \pm 2.0$	$12.0 \pm .8$	$39.3 \pm 1.3$
	9.7	c	15	$13\frac{1}{2}$	$41\frac{1}{2}$
	9.75*	$15\frac{1}{2}$	$15\frac{1}{2}$	12	41
	9.8	$15\frac{1}{2}$	$16\frac{1}{2}$	10	40
199	Exp.	c	c	$17.2 \pm 1.0$	$42.4 \pm .8$
	9.7	c	c	$18\frac{1}{2}$	$43\frac{1}{2}$
	9.8*	c	c	16	43
210	Exp.	c	c	$22. \pm 3.5$	$44.3 \pm 1.5$
	9.9	c	c	16	43
	10.0*	c	c	$19\frac{1}{2}$	45
	10.1	c	c	23	45
217	Exp.	$16.8 \pm .6$	$15.6 \pm .8$	$9.4 \pm .8$	-
	9.8	17	17	$6\frac{1}{2}$	
	9.9	17	17	8	
	10.0*	17	15	10	

Table IV continued

<sup>a</sup> See footnote a, Table III. Line widths used for spectra in this table are 1.8 cps (188°K), 1.9 (196), 2.1 (199), 3.2 (210), 2.2 (217), and 2.0 (238).

<sup>b,c</sup> Same as Table III.

---

---

determined by finding what value of this parameter, when used in the time average approximation, yielded the observed high temperature spectrum. The major experimental error in this calculation is the energy,  $E_3$ , of rotamer III, which introduces an uncertainty of about 11 cps in the value of  $(\nu_A - \nu_B)_{II}$ . Consistent results are obtained for the high temperature spectra for a range of chemical shifts and rotamer energies about the values used in the original calculation,  $E_3 = 746$  cal/mole and  $(\nu_A - \nu_B)_{II} = -11.0$  cps.

Increasing the temperature to  $154^\circ\text{K}$  coalesces lines 7-8 and 19-21 of rotamer II. At  $158^\circ\text{K}$  (Fig. 15) all the pairs of doublets have coalesced except peaks 12-15 and 22-24, which are shown in the experimental spectrum at a higher gain. The temperature must be increased above  $165^\circ\text{K}$  before these peaks coalesce. To calculate this feature it is clearly necessary that rotamer III be isolated from the other two rotamers, which are interchanging fairly rapidly at  $165^\circ\text{K}$ . The calculated spectra will only reproduce the experimental ones if both  $E_5$ , the barrier between rotamers II and III, and  $E_6$ , the barrier between rotamers III and I, are at least 8.8 kcal/mole. The observed width of peak 12,  $7 \pm 2$  cps at  $154^\circ\text{K}$ ,  $9 \pm 2$  at  $158^\circ\text{K}$ , and  $13 \pm 2$  at  $162^\circ\text{K}$ , can be reproduced either by taking  $E_5 = E_6$ , or choosing one of the two barriers higher than the other. Because exchange is occurring so rapidly between rotamers I and II, the calculated spectrum depends primarily on the total rate of exchange of I and II with III. At higher temperatures peaks 12-15 have coalesced with peaks 1-11. A large number of spectra were calculated at  $186^\circ$  and  $196^\circ$  in which  $E_5$  and  $E_6$  were separately varied in the range 9.0 to 10.5 kcal/mole. However, the spectra calculated with  $E_5$  not equal to  $E_6$  could

always be obtained with both barriers the same, at some intermediate value of  $E_5$  and  $E_6$ . For example, the calculated spectrum with  $E_5 = 10.0$  and  $E_6 = 9.0$  differs negligibly from the one with  $E_5 = E_6 = 9.1$  at  $186^\circ\text{K}$ . Consequently, in the discussion which follows all spectra were calculated with  $E_5$  equal to  $E_6$ .

The observed width of peak 12 is obtained with  $E_5 = 9.0$  at  $154^\circ\text{K}$ ,  $9.1$  at  $158^\circ\text{K}$ , and  $9.2$  kcal/mole at  $162^\circ\text{K}$ . This large variation is partially due to varying degrees of saturation of the peaks, which was necessary in order to observe them. Saturation introduces additional broadening of the peaks, so that the true widths should be narrower, and the actual energy slightly higher. The form of the rest of the spectrum is accurately reproduced with  $E_4 = 7.8$  kcal/mole at these three temperatures. In particular, at  $158^\circ$ , the width of peaks 5-6 is calculated to be  $38\frac{1}{2}$  cps for  $E_4 = 7.7$ , and 33 cps for  $E_4 = 7.8$ . The experimental value is  $34 \pm 2$  cps. At  $162^\circ$  (Fig. 16) the results for the width are 45 cps (7.7), 55 cps (7.8), and  $51 \pm 4$  cps (experimental). The frequency separations are unchanged, within experimental error, from those observed at  $150^\circ\text{K}$ . Note that decreasing  $E_5$  to 9.0 in Fig. 16 makes peaks 12-15 much broader.

The spectrum at  $165^\circ\text{K}$  is reproduced best with  $E_4 = 7.9$  and  $E_5 = 9.2$ . Increasing the temperature to  $171^\circ\text{K}$  coalesces peaks 12 and 13, and 14 and 15. The frequency separation between peaks 3-4 and 5-6 (the latter is the large peak at 400 cps on the scale in the figure) has decreased at this temperature to  $119 \pm 4$  cps, and this difference continues to decrease as the temperature is raised until it is only 21.7 cps at  $231^\circ\text{K}$ . At most intermediate temperatures it is a sensitive function of the barrier. For example, it is 102 cps for  $E_4 = 7.8$  and 116 cps for  $E_4 = 7.9$  at  $171^\circ$ .

The observed width, 61 cps for peaks 5-6, is somewhat larger than that calculated (47 cps for the 7.9 barrier). The splitting of peaks 16-18 into a triplet occurs at  $E_4 = 7.8$ ,  $E_5 = 9.2$  or  $E_4 = 7.9$ ,  $E_5 = 9.4$ . This shows exchange between rotamers I and II is occurring so rapidly that the fluorines are averaged. The triplet is coalesced again at  $186^\circ$  as the exchange with rotamer III becomes effective.

At  $186^\circ\text{K}$  the experimental frequency difference between peaks 3-4 and 5-6 is  $60 \pm 4$  cps, and the width of peak 5-6 is  $43 \pm 2$  cps. The calculated spectrum with  $E_4 = 8.1$  and  $E_5 = 9.0$  gives 64 and 46 cps, respectively. If  $E_4$  is between 7.6 and 8.0, then the frequency separation is 68 cps and the 400 cps peak is much sharper. The considerable discrepancy between the energies required to calculate the spectra at  $186^\circ$  compared to the other temperatures may be due to an abnormally large error in the temperature calibration.

An alternative explanation is the error in the energy of the third rotamer, which directly affects the chemical shifts of rotamer II used in the calculation. At  $186^\circ$  the exchange between I and II is rapid, so that the calculated chemical shifts are independent of  $E_4$  if it is less than 8.1. Exchange with III is sufficiently slow that the effect of  $E_5$  and  $E_6$  is slight. If  $E_3$  were 50 cal/mole higher, the calculated chemical shifts would be about 5 cps smaller at  $186^\circ\text{K}$ . At other temperatures a small adjustment in the barriers, about .1 kcal, changes the calculated chemical shifts sufficiently that an error in  $E_3$  would be unnoticed.

At  $196^\circ$  exchange between rotamers I and II is so rapid that the spectrum depends only on the value of  $E_5$ . The choice of  $E_5 = 9.2$  gives the best fit to the experimental spectrum, in which the experimental

and calculated chemical shift between peaks 3-4 and 5-6 are both 54 cps. However the width at half height of the large peak is calculated to be only 40 cps, whereas the experimental value is  $48 \pm 4$  cps. The width for the peak at 950 cps is calculated to be 47, and the experimental result is  $52 \pm 4$  cps. Changing the barriers does not make the peaks significantly broader, but does change the chemical shift by about 5 cps for each .1 kcal, so that the discrepancy between the observed and calculated width may again be due to a slight saturation of the peaks.

At  $205^\circ$  the barrier  $E_5$  is about 9.3 kcal. The AB part of the spectrum (from 200 to 600 cps) is becoming the usual octet of peaks for an ABX spectrum, and the X part of the spectrum sharpens into a triplet. The peak at 430 cps (on the scale in the figure) is due to the A fluorine in the notation used by Newmark and Sederholm.<sup>20</sup> Referring to Table I of their paper,  $\nu_A$  in the three rotamers at  $150^\circ\text{K}$  is 3438.8, 3474.5, and 3639.9 cps upfield from the solvent, respectively, whereas the chemical shifts for  $\nu_B$  are 3194.2, 3485.4 and 3859.2 cps. Thus the A fluorine resonates in three environments whose chemical shifts differ by only 200 cps, and should produce a much sharper signal than the B fluorine, in which the chemical exchange must be sufficient to average over three environments whose frequencies differ by 650 cps. The exchange rate must be three times faster for the B fluorine in order to make its peaks as sharp as those for the A fluorine. The splitting of the A peaks due to coupling with the  $F_X$  nucleus can also be observed at a lower temperature. This qualitatively explains the appearance of the spectra above  $180^\circ$ .

At 220°K the choice of  $E_5 = 9.5$  kcal/mole gives the best fit to the spectrum, reproducing the width of peak 5 ( $11. \pm 1$ . cps) and the peak 4-5 frequency difference of 26 cps. Increasing  $E_5$  to 9.6 coalesces peaks 3 and 4.

It has been possible to determine only the lowest barrier to internal rotation in  $\text{CF}_2\text{Br-CFBrCl}$ ,  $E_4 = 7.9 \pm .1$  kcal/mole. The experimental spectra can be reproduced choosing the two higher barriers equal to  $9.3 \pm .2$  kcal/mole. However, since the spectrum is only a function of the total rate of exchange with the third rotamer, it is impossible to determine the two other barriers separately. A lower limit of 8.8 can be set on them.

The three rotamers are drawn in Fig. 17. From steric considerations, rotamer I is assigned to drawing A, II to B, and III to C. Although the calculations are independent of this assignment, it can be used to determine the form of the activated complex for the three possible rotations. When the substituted methyl group,  $\text{CFClBr}$ , on A rotates 120 degrees to form rotamer B, it is necessary that the chlorine move past the fluorine, the bromine pass the second fluorine, and the fluorine pass the bromine. In the transition state these three pairs of atoms are presumably eclipsed. The results on  $\text{CF}_2\text{Br-CFBr}_2$  and  $\text{CF}_2\text{Br-CCl}_2\text{Br}$ , in which the assignment of the rotamers is unambiguous, indicate that if two large halogens, such as a bromine and chlorine or two bromines, are eclipsed, then the barriers are much larger. This evidence is reviewed below. In  $\text{CF}_2\text{Br-CFBrCl}$  it is seen that the AC and BC exchange requires eclipsing two large halogens. The assignment made above is then completely consistent with the barrier determination since  $E_4$ , the lowest barrier, is between rotamers I and II, or A and B.

$\text{CF}_2\text{Br-CHBrCl}$

$\text{CF}_2\text{Br-CHBrCl}$  was studied as an approximately 25% by volume solution in  $\text{CF}_2\text{Cl}_2$ . The low temperature fluorine spectrum is shown in Fig. 18. The spectrum should consist of the superposition of three AB quartets, one for each rotamer; and each line should be a doublet from the H-F splitting. In analogy to  $\text{CF}_2\text{Br-CFBrCl}$  and  $\text{CF}_2\text{Br-CFBr}_2$ , the AB coupling constant should be about 165 cps. The spectrum is substantially different from that of  $\text{CF}_2\text{Br-CFBrCl}$ , and the assignment was finally made by a careful consideration of the relative areas of the peaks. Peaks 1, 2, 6, 7, 10, and 11 are assigned to the AB quartets of rotamer I, peaks 3, 4, 8, 9, 12, and 13 to the AB quartets of rotamer III, and the remaining peak, number 5, to rotamer II. The two fluorines are nearly degenerate in this rotamer. Peaks 1 through 4 should be doublets, but no splitting was ever observed on these peaks, indicating that two of the HF coupling constants are almost zero. Peak 5 was obtained as a quartet on two occasions; the four peaks are 2602.2, 2604.6, 2607.5, and 2610.3 cps upfield from the solvent. The 146°K proton spectrum consists of two broad, overlapping peaks.

The spectra of the three rotamers were analyzed as ABX spectra to obtain the chemical shifts. Although all the H-C-C-F coupling constants that have been reported have the same sign,<sup>25</sup> the results have only been obtained in substituted ethanes at room temperature, and on one substituted ethylene. The data presented here suggests the coupling constants at room temperature are the superposition of large values for some rotamers and small ones in the others. In particular, the small coupling constants may have the opposite sign of the large ones. We have assumed both coupling constants are positive in rotamer II. The coupling constants in



rotamers I and III were taken directly from the observed splittings. The results are in Table V.

The spectrum has been analyzed at 229°K and 303°K where averaged chemical shifts and coupling constants are observed. These are also listed in Table V. The spectrum at 303°K is exactly analogous to peaks 1-8 in Fig. 11 for the AB peaks of rotamer I of  $\text{CF}_2\text{Br}-\text{CFBr}_2$  in which the peaks in each doublet have the same intensity. Consequently the two HF coupling constants must have the same sign at 303°K. From the qualitative application of the time average approximation to the coupling constants it then follows that the two large coupling constants in rotamers I and III have the same sign. The energies of the rotamers were obtained from the average of several integral spectra -  $E_2 = 167 \pm 13$  cal/mole and  $E_3 = 248 \pm 20$  cal/mole.

The averaged coupling constants and chemical shifts at high temperatures have been calculated from the time average approximation.<sup>20</sup> The unobserved coupling constants were assumed to be zero. The results are in Table VI. The calculated coupling constants are larger than the observed ones (in Table V) by approximately the same amount as the results obtained in  $\text{CF}_2\text{Br}-\text{CFBrCl}$ .<sup>20</sup> The discrepancy would be larger if some finite values were assumed for the near-zero coupling constants. In any case, the trend of the two coupling constants is quantitatively reproduced. The calculated value of the chemical shift between the two fluorines on the same carbon is within experimental error of the observed values. The observed discrepancies between the calculated and observed shift from the solvent peak are the usual order of magnitude. These results substantiate the conclusions drawn from the  $\text{CF}_2\text{Br}-\text{CFBrCl}$  chemical shift data by Newmark and Sederholm.<sup>20</sup>

Table V

Chemical shifts and coupling constants for the three rotamers of  $\text{CF}_2\text{Br-CHBrCl}$  at  $123^\circ\text{K}$ , and of the averaged spectrum at  $229^\circ\text{K}$  and  $303^\circ\text{K}$ . All values are in cycles per second.

	$J_{\text{AB}}$	$J_{\text{AX}}$	$J_{\text{BX}}$	$\nu_{\text{A}}^{\text{a}}$	$\nu_{\text{B}}^{\text{a}}$	$\nu_{\text{B}} - \nu_{\text{A}}^{\text{a}}$
I	$160.8 \pm .5$	<2.	$18.9 \pm .3$	2268.4	3298.8	1030.4
II	-	$1.8 \pm .4$	$3.4 \pm .4$	2584.3	2628.2	42.9
III	$159.0 \pm .7$	$18.5 \pm 1.0$	<2.	3374.8	2467.4	-907.4
$229^\circ\text{K}$	$161.6 \pm .4$	$5.2 \pm .3$	$8.9 \pm .3$	2630.8	2862.5	231.7
$303^\circ\text{K}$	$162.2 \pm .4$	$5.65 \pm .2$	$8.6 \pm .2$	2631.3	2819.1	187.8

<sup>a</sup> The root-mean square deviation in the chemical shifts is 2.0 for rotamers I and III, 5.0 for II, 0.7 at  $229^\circ\text{K}$ , and 0.5 at  $303^\circ$ .

146

Table VI

Calculated chemical shifts and coupling constants (in cps)  
at high temperatures using weighted averages of the low  
temperature data for  $\text{CF}_2\text{Br-CHBrCl}$ .

	$J_{\text{AX}}$	$J_{\text{BX}}$	$\nu_{\text{A}}$	$\nu_{\text{B}} - \nu_{\text{A}}$
229°K	5.3	9.3	2647.6	233.7
303°	5.7	8.8	2672.1	187.6

The spectra at intermediate rates of exchange are shown in Fig. 19. The situation is analogous to the experimental results of  $\text{CF}_2\text{Br-CFBrCl}$ - the peaks of one rotamer, in this case rotamer II, are not broadened by exchange whereas the other two rotamers are undergoing rapid exchange. Barriers  $E_4$  and  $E_5$  must be at least 7.8 kcal/mole to calculate the experimental spectrum with a sharp peak 5. The choice of  $E_6 = 6.9$  kcal/mole (Fig. 20) gives the observed width,  $70 \pm 10$  cps, for peak 2 in the figure at  $147^\circ\text{K}$  (the peaks are numbered according to Fig. 18).

Spectra were calculated with  $E_4$  equal to  $E_5$  since the previous results on  $\text{CF}_2\text{Br-CFBrCl}$  showed that the spectra will only depend on the total rate of exchange of II with III or I.

The choice of  $E_4 = E_5 = 8.2$  kcal/mole at  $147^\circ\text{K}$  reproduces the observed width of the sharp peak,  $13\frac{1}{2}$  cps. Changing  $E_4$  by .1 kcal changes the width by less than a cycle at this low temperature.

When the temperature is increased to  $156^\circ$  the small peaks become extremely broad.  $E_4 = 8.1$  reproduces the width of the main peak,  $26 \pm 2$  cps;  $E_6$  between 6.7 and 6.9 reproduces the general appearance of the spectrum for this value of  $E_4$ . At  $168^\circ$  another peak  $385 \pm 20$  cps upfield from the main peak is observed.  $E_4 = 8.0$  reproduces the width of the large peak,  $165 \pm 20$  cps, and the observed chemical shift. Changing  $E_6$  has a small effect on the width.

At  $190^\circ\text{K}$  the AB part of an ABX spectrum is observed, in which the downfield pair of peaks are much sharper than the upfield pair. This appearance is explained in exactly the same manner as the  $\text{CF}_2\text{Br-CFBrCl}$  spectra above  $180^\circ$ . The observed spectrum is reproduced with  $E_4 = 8.2$ ,  $E_6 = 6.9$ , or  $E_4 = 8.1$ ,  $E_6 = 7.0$ . Both barriers have a noticeable effect

on the spectrum.  $E_6$  is still important at this relatively high temperature because of the large chemical shift between rotamers I and III.

At  $210^\circ$  the experimental spectrum can be reproduced for values of  $E_4$  about 8.2 and  $E_6$  about 6.9. The changes in the widths upon small variations of these parameters is insufficient to choose an exact value of the barrier at this temperature.

In conclusion, the lower barrier in  $\text{CF}_2\text{Br-CHBrCl}$  is  $6.9 \pm .2$  kcal/mole, and the higher barriers are at least 7.8 kcal/mole. The experimental spectra can be reproduced by choosing the higher barriers the same, and equal to 8.2 kcal/mole.

If steric hindrance of the bromines determines the relative stability of the rotamers, then drawing A of Fig. 21 is assigned as rotamer I, B as II, and C as III. In this case no simple explanation for the variation of the HF coupling constants is possible. However, only drawings A and B have the proton trans to a fluorine, and the probable explanation for the observed spectrum is that the four gauche H-F coupling constants are small and the two trans couplings large. Then drawing A is assigned to rotamer I, C to II, and B to III.  $F_A$  is a doublet in rotamer I,  $F_B$  a doublet in rotamer III, and the chemical shift relationships in Table V are satisfied.

The barriers to internal rotation show unequivocally that the barrier between rotamers I and III is over 1 kcal/mole less than the other two barriers. From the steric considerations discussed in the section on  $\text{CF}_2\text{Br-CFBrCl}$ , the activated complex for the lowest barrier should have the fluorines and the proton each eclipsing a larger halogen. Therefore the lowest barrier is between the rotamers represented by drawings A

and B in Fig. 21. Rotamer C must be assigned to peak 5, or rotamer II. This shows that the second assignment of rotamers to the drawings is correct, and presumably that the trans H-F coupling constants are substantially larger than the gauche ones. Since the coupling is transmitted through the bonds, it is unlikely that it should have extreme fluctuations with small changes in dihedral angle.

This interpretation of the coupling constant is supported by other evidence. Abragam and Bernstein<sup>26</sup> have studied the temperature dependence of  $J_{HF}$  in  $CFCl_2-CHCl_2$ . Although they were unable to reach a low enough temperature to freeze out the rotamers, the results could be explained by fitting the observed averaged coupling constant with  $E_2 = E_3 = 400$  cal/mole.  $J_{trans} = 18$  cps, and  $J_{gauche} = 1$  cps. Although it has been shown that this method of analysis is not quantitative,<sup>20,27</sup> the results in Table VI show that it should be qualitatively correct for these cases where the coupling constants in the low temperature rotamers are very different.

Fessenden and Waugh,<sup>28</sup> from a similar study of  $CHCl_2-CF_2Cl$ , find two sets of coupling constants for the two rotational isomers of the compound which when substituted into the time average approximation yield the observed results. The solution in which the more stable rotamer has all the chlorines gauche to one another (similar to drawing C in Fig. 21) gives  $J_{trans} = 10$  and  $J_{gauche} = 5$  cps. The results on  $CF_2Br-CHBrCl$  studied here indicate this assignment of the relative stability of the rotamers is likely to be correct. The alternative assignment for the relative stabilities gives a gauche coupling constant larger than the trans one.

The relative energies of the rotamers may be explained by a consideration of the dipole moment of the C-H and C-halogen bonds. The C-H dipole is much less than the C-halogen dipole, so that the dipole moment perpendicular to the C-C axis in rotamer C should be less than in rotamer B. This effect could be studied by determining the relative energies of the three rotamers of  $\text{CF}_2\text{Br-CHBrCl}$  in solvents of different dielectric strength.

## Discussion

### A. Chemical Shifts

The chemical shifts between two fluorine atoms on the same carbon varies by more than 15 ppm in the molecules discussed. Although this seems rather large, similar differences are obtained for methylene fluorines in cyclic compounds.<sup>29</sup> The results on  $\text{CF}_2\text{Br-CFBrCl}$  and  $\text{CF}_2\text{Br-CHBrCl}$  indicate that the smaller values usually observed in molecules undergoing free rotation result from an averaging of larger values of different signs in the various configurations.

That the spectrum of the three rotamers of  $\text{CF}_2\text{Br-CHBrCl}$  is very different from the one of  $\text{CF}_2\text{Br-CFBrCl}$  shows that substitution of a proton for a fluorine has a large effect on the electron distribution of the molecule. This is certainly reasonable in view of the change in magnitude of the dipole moment for the C-F compared to the C-H bond.

No correlation between the substituents gauche to the AB fluorines and their relative chemical shift has been noticed. Thus, in isomer I of  $\text{CF}_2\text{Br-CFBr}_2$  (Fig. 10) one of the fluorines is gauche to a fluorine and bromine, and the other gauche to two bromines. The two equivalent fluorines in isomer III are gauche to a fluorine and a bromine, yet

their resonance is several hundred cycles upfield from the resonance of I. Similar results are true for the other compounds. The distortion of the molecule from tetrahedral symmetry, due to the large bromine substituents, may be the main source of changes in the chemical shift between rotamers. In all the molecules studied the resonance of the fluorines in the high energy form are at higher magnetic field. The high energy form probably has the bromines gauche, and consequently the greatest distortion. This is definitely the case in  $\text{CF}_2\text{Br}-\text{CCl}_2\text{Br}$  and  $\text{CF}_2\text{Br}-\text{CFBr}_2$  where the two isomers have different spectra. In the other molecules it is impossible to assign the rotamers to the spectrum from such considerations because each rotamer has an ABX spectrum. However, in analogy to the first two molecules, and other halogenated ethanes, which have been studied by different techniques,<sup>30</sup> the highest energy form probably has the largest substituents gauche to each other. This is reasonable from steric and dipole moment considerations for the perhalogenated ethanes. This assignment was made in  $\text{CFClBr}-\text{CFClBr}$  and  $\text{CF}_2\text{Br}-\text{CFBrCl}$  in order to correlate the barriers in the next section. The assignment of  $\text{CF}_2\text{Br}-\text{CHBrCl}$  is apparently an exception to the usual rule that the high energy form has the large halogens gauche to each other.

In  $\text{CF}_2\text{Br}-\text{CFBr}_2$  and  $\text{CF}_2\text{Br}-\text{CFBrCl}$  there is some consistency in the resonance of the single upfield fluorine ( $\text{F}_X$ ). In the two rotamers (III in Fig. 10 and C in Fig. 17, respectively) where this fluorine is gauche to the two other fluorines it is several hundred cycles upfield from the resonance when the fluorine is gauche to a fluorine and a bromine or chlorine.



### B. Barriers

The free energies of activation, termed for simplicity the barriers, of the halogenated ethanes which have been determined in this work are listed in Table VII. The free energies are measured from the potential minimum of the most stable rotamer. The barriers of four additional perhalogenated ethanes, determined from infrared and electron diffraction measurements, have also been listed for comparison. Presumably the large barriers for the ethanes with bulky substituents like chlorine or bromine are steric in origin, and one would anticipate a correlation between the size of the substituent and the barrier. To show this correlation, the pairs of atoms which are eclipsed in the activated complex when the rotation occurs are also indicated in the Table.

Comparing the results in the compounds with two fluorines to those with three fluorines, it is clear that adding a bulky chlorine or bromine significantly increases the barrier.

The geometry of the molecule substantially affects the magnitude of the barriers. Thus,  $E_4$  in  $\text{CF}_2\text{Br}-\text{CCl}_2\text{Br}$  has exactly the same pairs of atoms eclipsed in the activated complex as  $E_4$  in  $\text{CFClBr}-\text{CFClBr}$ , yet the two barriers differ by .7 kcal./mole. There is a similar lack of agreement between  $E_5$  of the former molecule and  $E_5$  of the latter, although the experimental error is greater in this case. Although the  $\text{CFClBr}-\text{CFClBr}$  measurements were performed in  $\text{CS}_2$  solution while the  $\text{CF}_2\text{Br}-\text{CCl}_2\text{Br}$  measurements were made in  $\text{CFCl}_3$ , sufficient measurements of the latter compound in  $\text{CS}_2$  showed that the lower barrier did not change with solvent. The higher barriers in  $\text{CF}_2\text{Br}-\text{CCl}_2\text{Br}$  may be explained by observing that one of the carbons has three bulky substituents in this isomer. Distorting

Table VII

The pairs of atoms which are eclipsed in a rotation, and the associated free energy of activation, in kcal/mole.

Molecule	Barrier	Eclipsed Pairs
$\text{CF}_2\text{Br}-\text{CCl}_2\text{Br}$	$E_4 = E_6 = 10.8 \pm .1$	Br-Cl, Br-F, Cl-F.
	$E_5 \Rightarrow 12.0 \pm .5$	Br-Br, 2 Cl-F.
$\text{CFCl}_2-\text{CFCl}_2$	$E = 9.65 \pm .1$	Cl-Cl, 2 Cl-F.
$\text{CFClBr}-\text{CFClBr}$	$E_4 = E_6 = 10.1 \pm .2$	Br-Cl, Br-F, Cl-F.
	$E_5 \Rightarrow 12.0 \pm 1.0$	Br-Br, Cl-Cl, F-F.
	$E'_4 = 9.9 \pm .2$	2 Br-F, Cl-Cl.
	$E'_5 \Rightarrow 10.6 \pm .2$	Br-Br, 2 Cl-F.
	$E'_6 \Rightarrow 10.6 \pm .2$	2 Br-Cl, F-F.
$\text{CF}_2\text{Br}-\text{CFBr}_2$	$E_4 = 7.7 \pm .2$	3 Br-F.
	$E_5 = E_6 = 9.9 \pm .2$	Br-Br, Br-F, F-F.
$\text{CF}_2\text{Br}-\text{CFBrCl}$	$E_4 = 7.9 \pm .1$	2 Br-F, Cl-F.
	$E_5 \Rightarrow 8.8$	Br-Br, Cl-F, F-F.
	$E_6 \Rightarrow 8.8$	Br-Cl, Br-F, F-F.
$\text{CF}_2\text{Br}-\text{CHBrCl}$	$E_4 \Rightarrow 7.8$	Br-Cl, Br-F, F-H.
	$E_5 \Rightarrow 7.8$	Br-Br, Cl-F, F-H.
	$E_6 = 6.9 \pm .2$	Br-F, Br-H, Cl-F.

Table VII continued

Molecule	Barrier	Eclipsed Pairs
$\text{CF}_3\text{CF}_3^{\text{a}}$	E = 4.35	3 F-F.
$\text{CF}_3\text{-CF}_2\text{Cl}^{\text{b}}$	E = 5.67	Cl-F, 2 F-F.
$\text{CF}_3\text{-CF}_2\text{Br}^{\text{b}}$	E = 6.4	Br-F, 2 F-F.
$\text{CCl}_3\text{-CCl}_3^{\text{c}}$	E = 10.8 ± 3.	3 Cl-Cl.

<sup>a</sup> Reference 2.

<sup>b</sup> Reference 5.

<sup>c</sup> Reference 3.

the bond angles from tetrahedral symmetry to move the bromines further apart in the eclipsed state is then rendered more difficult.

It is reasonable that the barrier will be the sum of three terms, corresponding to the three pairs of eclipsed atoms in the activated complex. Let  $E(\text{Br-F})$  denote the contribution to the total barrier of a bromine atom and a fluorine atom which are eclipsed. It is possible to obtain barrier contributions from each pairwise interaction, although the conclusions already drawn show these may have little significance. It is nevertheless interesting to obtain an independent result from the other molecules studied. From the  $\text{CF}_3\text{-CF}_3$  and  $\text{CF}_3\text{-CF}_2\text{Br}$  results,  $E(\text{F-F}) = 1.45$  kcal./mole, and  $E(\text{F-Br}) = 3.50$  kcal./mole. However  $E(\text{F-Br}) = 2.75$  kcal./mole is calculated from  $E_4$  of  $\text{CF}_2\text{Br-CFBr}_2$ , 25% lower than 3.50. Further consideration of pairwise contributions to the barrier in different molecules is clearly unwarranted.

It is interesting that the two barriers in an asymmetric compound are significantly different (2.2 kcal./mole in  $\text{CF}_2\text{Br-CFBr}_2$ ). A theory to quantitatively predict the results cannot depend linearly on the size of the substituents. Thus,  $E(\text{Br-Br}) + E(\text{F-F}) \neq 2 E(\text{Br-F})$ . In Table VIII the distance from a substituent on an ethane to the plane bisecting the carbon-carbon bond is given. These values can be compared to the Van der Waals radii, also given in the Table. The bromine and chlorine Van der Waals radii extend much further than the bisecting plane. The overlap of the eclipsed atoms, corresponding to  $E(\text{Br-Br})$ ,  $E(\text{F-F})$ , and  $E(\text{Br-F})$ , are 1.06, .24, and .65 Å, respectively. A linear theory would postulate that the barrier contribution is directly proportional to this overlap, and conclude that  $E_4 = E_5$  in  $\text{CF}_2\text{Br-CFBr}_2$ . However the results prove that the

Table VIII

The distance from a halogen or proton substituted on an ethane to the plane bisecting the carbon-carbon bond,  $D$ , and its Van der Waals radius  $R$ . All distances are in Angstroms.

Substituent	C-X distance <sup>a</sup>	$D^b$	$R^c$	$D - R$
H	1.095	1.13	1.2	-0.07
F	1.375	1.23	1.35	-0.12
Cl	1.78	1.36	1.80	-0.44
Br	1.94	1.42	1.95	-0.53

<sup>a</sup> From L. E. Sutton, "Table of Interatomic Distances and Configurations in Molecules and Ions," The Chemical Society, London, 1958.

<sup>b</sup> The calculation assumes tetrahedral bond angles.

<sup>c</sup> L. Pauling, "The Nature of the Chemical Bond," Cornell University Press, Ithaca, New York, 1960, p. 260.

barrier is proportional to some power of the overlap distance. In fact the overlap is so great that some distortion of the carbon bonding orbitals undoubtedly occurs to reduce it in the transition state, which eliminates simple correlations of the data. In this respect, it is interesting to note that the distance between two bromines on a tetrahedral carbon atom is 3.17 Å, or .34 Å further apart than the two eclipsed bromines.

The series of compounds,  $\text{CF}_2\text{Br}-\text{CClBrX}$ ,  $X = \text{H}, \text{F}, \text{and Cl}$  has been studied. A significant increase, 1.0 kcal./mole, in the magnitude of the barrier occurs with substitution of a fluorine for a proton. This substantial increase in the barrier may be a steric effect. In one case the bromine is eclipsed with a proton, in the other case with a fluorine. In addition a contributing factor to the difference may be the change in the magnitude, and possibly direction, of the bond dipole upon substitution of the fluorine for the proton. Changing the fluorine to a chlorine increases the barrier even more, by 3.0 kcal./mole. The significant increase in the barrier with substitution of a chlorine occurs because in  $\text{CF}_2\text{Br}-\text{CCl}_2\text{Br}$  any rotation requires that two large halogens be eclipsed.

Finally, the free energies of activation are independent of temperature, within experimental error. The results presented show the theory is sufficiently sensitive to small changes in the barriers that it should be possible to measure the temperature dependence of the barriers with experimental apparatus which provide more accurate temperature control. The error in the barrier is directly proportional to the absolute error in the temperature because of the exponential dependence of the rate laws used in this work.

Summary

The results on  $\text{CF}_2\text{Br}-\text{CCl}_2\text{Br}$  and  $\text{CF}_2\text{Br}-\text{CFBr}_2$  have been presented in considerable detail to show that the modification of the theory of exchange developed above can accurately reproduce experimental spectra. For the more complex molecules studied it was impossible to obtain the free energies of activation between all three rotamers. However, the theory is still capable of reproducing the observed spectra within experimental error in the parameters used in the calculation.

The listings and write-up for the computer programs are available upon request.<sup>15</sup>

Acknowledgements: We thank the U.S. Atomic Energy Commission through the Inorganic Materials Research Division of the Lawrence Radiation Laboratory for support of this work. One of us (R. A. N.) gratefully acknowledges Fellowship aid from the National Science Foundation.

References

1. E. B. Wilson, Jr., *Advan. Chem. Phys.* 2, 367 (1959).
2. E. L. Pace, *J. Chem. Phys.* 16, 74 (1948).
3. Y. Morino and E. Hirota, *J. Chem. Phys.* 28, 185 (1958).
4. C. R. Ward and C. H. Ward, *J. Mol. Spec.* 12, 289 (1964).
5. O. Risgin and R. C. Taylor, *Spectrochim. Acta.* 15, 1036 (1959).
6. D. S. Thompson, R. A. Newmark, and C. H. Sederholm, *J. Chem. Phys.* 37, 411 (1962).
7. H. M. McConnell, *J. Chem. Phys.* 28, 430 (1958).
8. J. I. Kaplan, *J. Chem. Phys.* 28, 278 (1958).
9. (a) S. Alexander, *J. Chem. Phys.* 37, 967 (1962); (b) 37, 974 (1962).
10. J. I. Kaplan, *J. Chem. Phys.* 29, 462 (1958).
11. R. J. Kurland and W. B. Wise, private communication.
12. J. Heidberg, J. A. Weil, G. A. Janusonis, and J. K. Anderson, *J. Chem. Phys.* 41, 1033 (1964).
13. C. S. Johnson, *J. Chem. Phys.* 41, 3277 (1964).
14. R. A. Newmark, Thesis, University of California, Berkeley, November, 1964; or Lawrence Radiation Laboratory Report UCRL 11649, 1964, University of California, Berkeley, California (unpublished).
15. The computer program, written in Fortran IV, is available on request to C. H. Sederholm.
16. S. Glasstone, K. Laidler, and H. Eyring, "The Theory of Rate Processes," (McGraw-Hill Book Co., Inc., New York, 1941).
17. A. A. Frost and R. G. Pearson, "Kinetics and Mechanism," (John Wiley and Sons, New York, 1961), p. 130.



18. S. W. Benson, "The Foundations of Chemical Kinetics," (McGraw-Hill Book Co., Inc., New York, 1960) Chapter XV.
19. F. W. Cagle, Jr. and H. Eyring, J. Am. Chem. Soc. 73, 5628 (1951).
20. R. A. Newmark and C. H. Sederholm, J. Chem. Phys. 39, 3131 (1963).
21. G. V. D. Tiers, J. Phys. Chem. 67, 928 (1963).
22. H. S. Gutowsky and C. H. Holm, J. Chem. Phys. 25, 1228 (1956).
23. S. L. Manatt and D. D. Elleman, J. Am. Chem. Soc., 84, 1305 (1962).
24. W. S. Brey, Jr., and K. C. Ramey, J. Chem. Phys. 39, 3546 (1963).
25. D. F. Evans, S. L. Manatt, and D. D. Elleman, J. Am. Chem. Soc. 85, 238 (1963).
26. R. J. Abragam and H. J. Bernstein, Can. J. Chem. 39, 39 (1961).
27. R. J. Abragam and L. Cavalli, Mol. Phys., to be published.
28. R. W. Fessenden and J. S. Waugh, J. Chem. Phys. 37, 1466 (1962).
29. J. A. Pople, W. G. Schneider, and J. H. Bernstein, "High Resolution Nuclear Magnetic Resonance," (McGraw-Hill Book Co., Inc., New York, 1959), Chapter XII.
30. S. Mizushima, "Structure of Molecules and Internal Rotation," (Academic Press, Inc., New York, 1954), Chapters II and III.

Figure Captions

- Figure 1. A possible potential energy curve as a function of dihedral angle.
- Figure 2. Experimental spectrum of  $\text{CF}_2\text{Br}-\text{CCl}_2\text{Br}$  at  $191^\circ\text{K}$ .
- Figure 3. The three rotamers of  $\text{CF}_2\text{Br}-\text{CCl}_2\text{Br}$ .
- Figure 4. Experimental spectra of  $\text{CF}_2\text{Br}-\text{CCl}_2\text{Br}$  at several temperatures ( $^\circ\text{K}$ ). The zero point on the frequency scale has been adjusted according to Eq. (18), and set 3112.6 cps upfield from the solvent. The sharp peaks on either side of the experimental spectra are sidebands of the solvent,  $\text{CFCl}_3$ .
- Figure 5. Experimental and calculated spectra of  $\text{CF}_2\text{Br}-\text{CCl}_2\text{Br}$  at  $222\frac{1}{2}^\circ\text{K}$ .
- Figure 6. The three rotamers of each isomer of  $\text{CFClBr}-\text{CFClBr}$ .
- Figure 7. Experimental spectrum of  $\text{CFClBr}-\text{CFClBr}$  at  $177^\circ\text{K}$ .
- Figure 8. Experimental and calculated spectra of  $\text{CFClBr}-\text{CFClBr}$  at  $194^\circ\text{K}$ .
- Figure 9. Spectra of  $\text{CFCl}_2\text{CFCl}_2$  in  $\text{CFCl}_3$  at several temperatures ( $^\circ\text{K}$ ). The sharp peaks on the left and right of each spectrum are sidebands of the solvent, at 3780 and 3928 cps at  $186\frac{1}{2}^\circ$ , 3752 and 3956 cps at  $196\frac{1}{2}^\circ$ , 3805 and 3916 cps at  $200^\circ$ , and 3794 and 3943 cps at all other temperatures.
- Figure 10. The three rotamers of  $\text{CF}_2\text{Br}-\text{CFBr}_2$ .
- Figure 11. Experimental spectrum of  $\text{CF}_2\text{Br}-\text{CFBr}_2$  at  $152^\circ\text{K}$ .
- Figure 12. Experimental spectra of  $\text{CF}_2\text{Br}-\text{CFBr}_2$  at several temperatures ( $^\circ\text{K}$ ). The zero on the frequency scale is arbitrarily located about 3000 cps upfield from the solvent,  $\text{CF}_2\text{Cl}_2$ ; the exact value is chosen such that peak 5 is located at the same point

as its calculated location from the computer spectra. The sharp peaks on the sides of several of the spectra are solvent sidebands. The spectra on the left are of the peak 3-6 region; those on the right of the peak 11-13 region.

Figure 13. Experimental and calculated spectra of  $\text{CF}_2\text{Br-CFBr}_2$  at  $167^\circ\text{K}$ .

Figure 14. Spectrum of  $\text{CF}_2\text{Br-CFBrCl}$  at  $150^\circ\text{K}$ . The separation between peaks 1 and 24 is 1243 cps.

Figure 15. Spectra of  $\text{CF}_2\text{Br-CFBrCl}$  at several temperatures ( $^\circ\text{K}$ ). The sharp peaks on either side of each spectrum are sidebands of the solvent,  $\text{CFCl}_3$ .

Figure 16. Experimental and calculated spectra of  $\text{CF}_2\text{Br-CFBrCl}$  at  $162^\circ\text{K}$ . Solvent sidebands are at 2902 and 4146 cps.

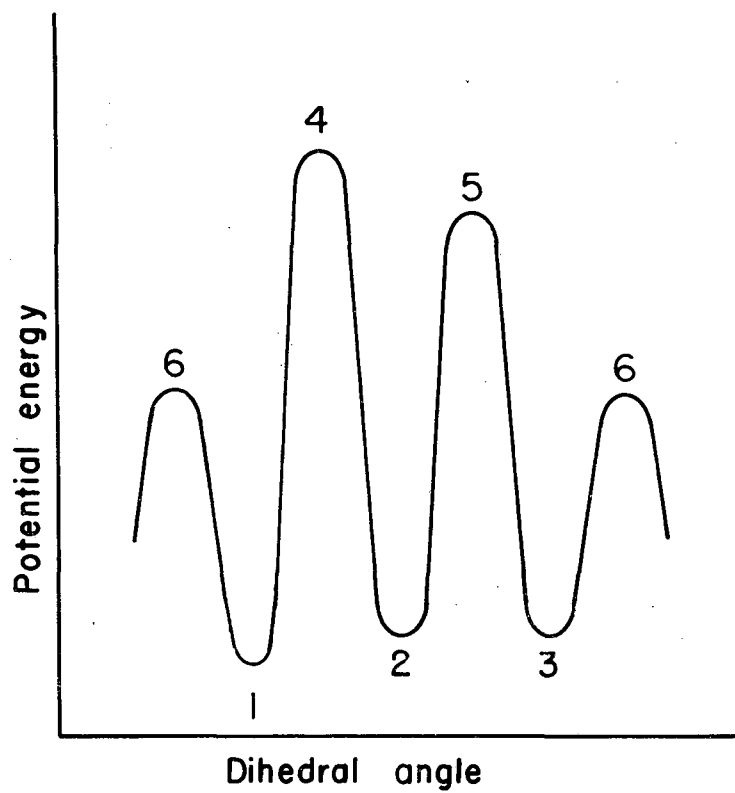
Figure 17. The three rotamers of  $\text{CF}_2\text{Br-CFBrCl}$ .

Figure 18. Experimental spectrum of  $\text{CF}_2\text{Br-CHBrCl}$  at  $123^\circ\text{K}$ .

Figure 19. Spectra of  $\text{CF}_2\text{Br-CHBrCl}$  at several temperatures ( $^\circ\text{K}$ ). The sharp peaks on either side of each spectrum are sidebands of the solvent,  $\text{CF}_2\text{Cl}_2$ .

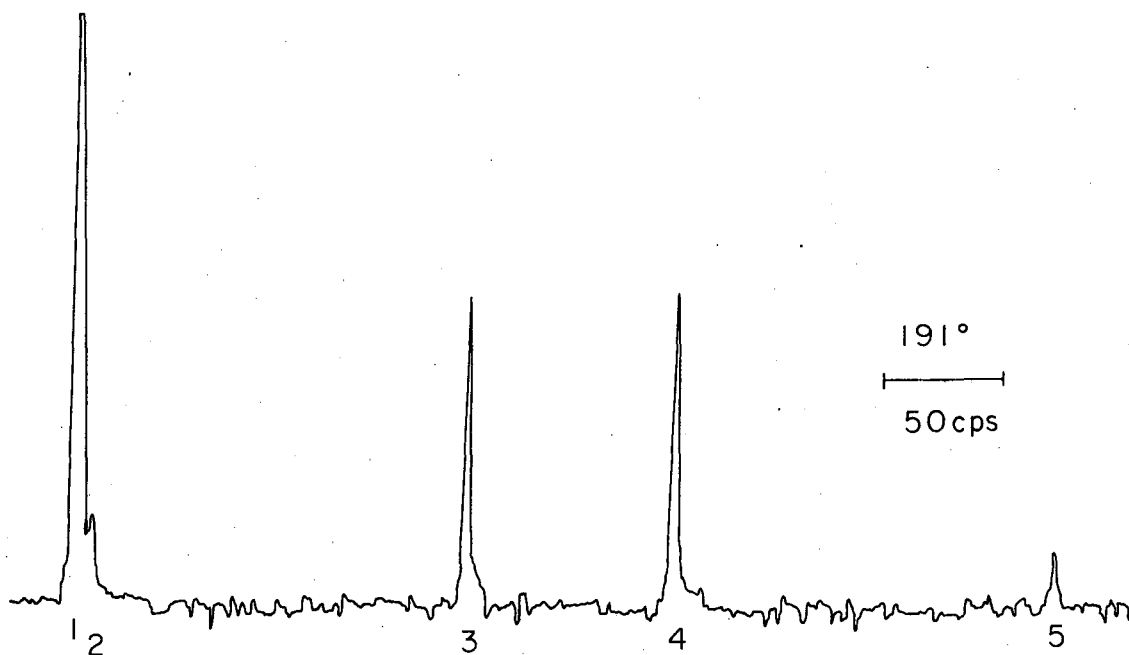
Figure 20. Experimental and calculated spectra of  $\text{CF}_2\text{Br-CHBrCl}$  at  $147^\circ\text{K}$ . Solvent sidebands are at 1947 and 3749 cps.

Figure 21. The three rotamers of  $\text{CF}_2\text{Br-CHBrCl}$ .



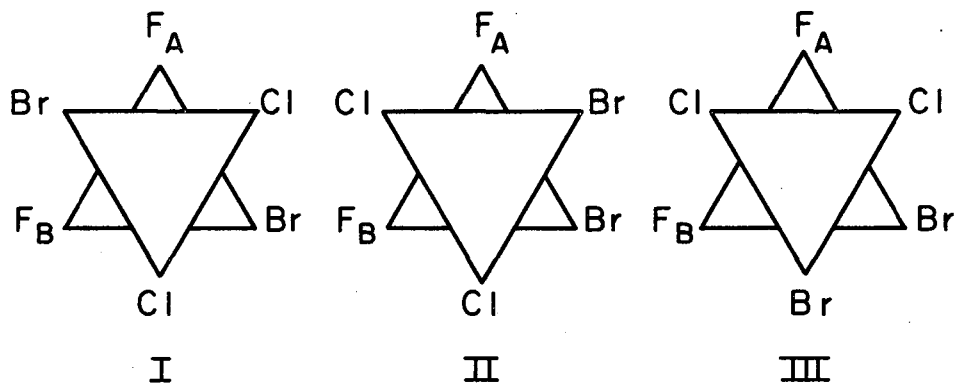
MU-34831

Fig. 1



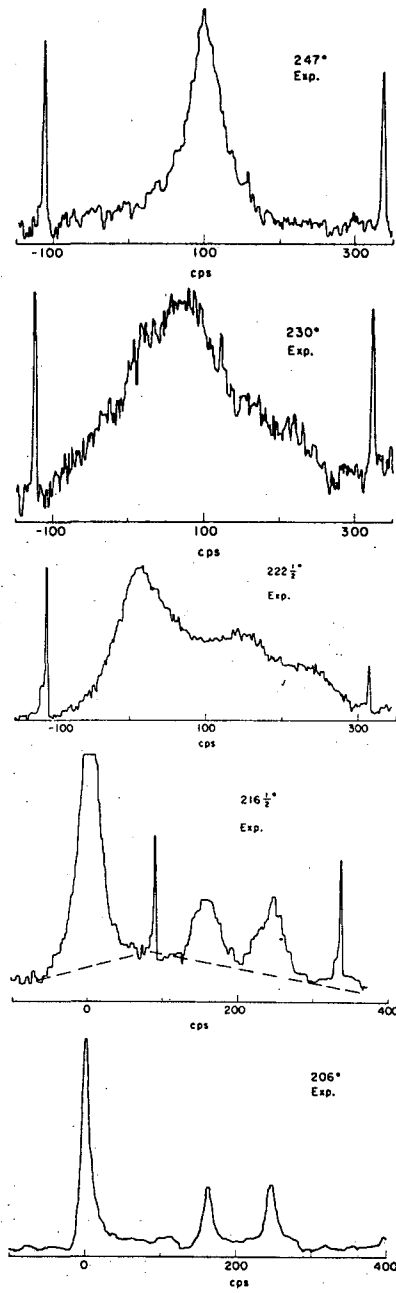
MU.34832

Fig. 2



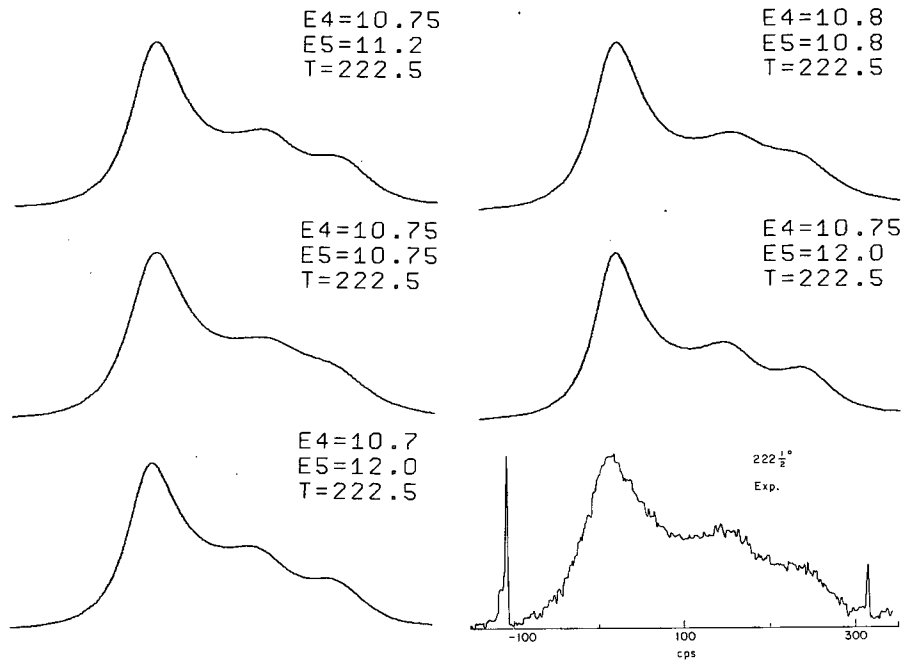
MU-34821

Fig. 3



MUB-4408

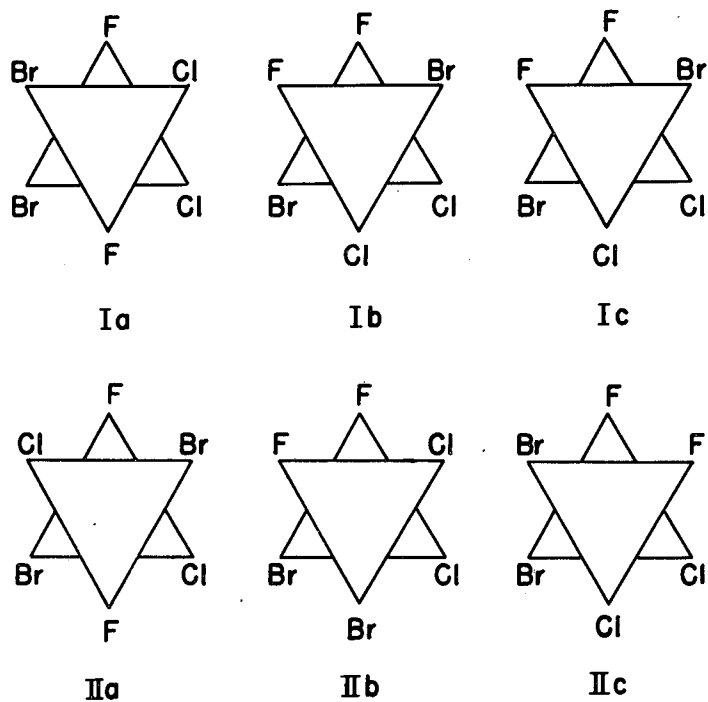
Fig. 4



MU-34868

Fig. 5





MU - 24684

Fig. 6

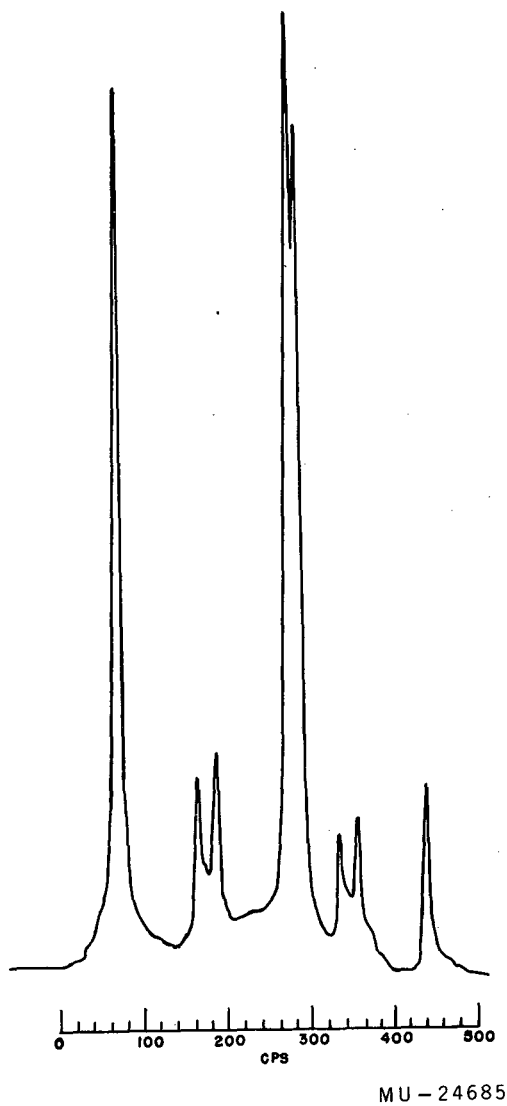
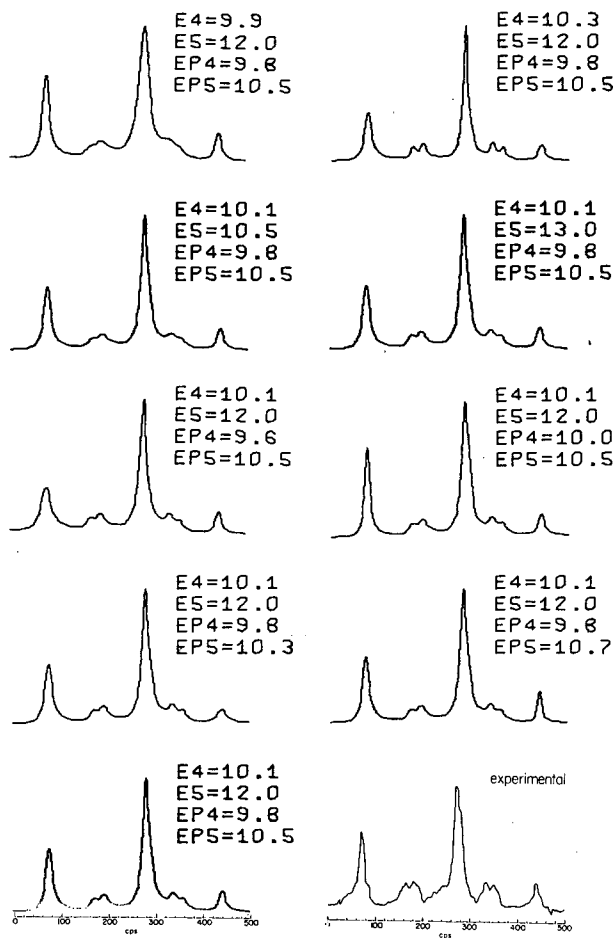


Fig. 7



MU-34837

Fig. 8

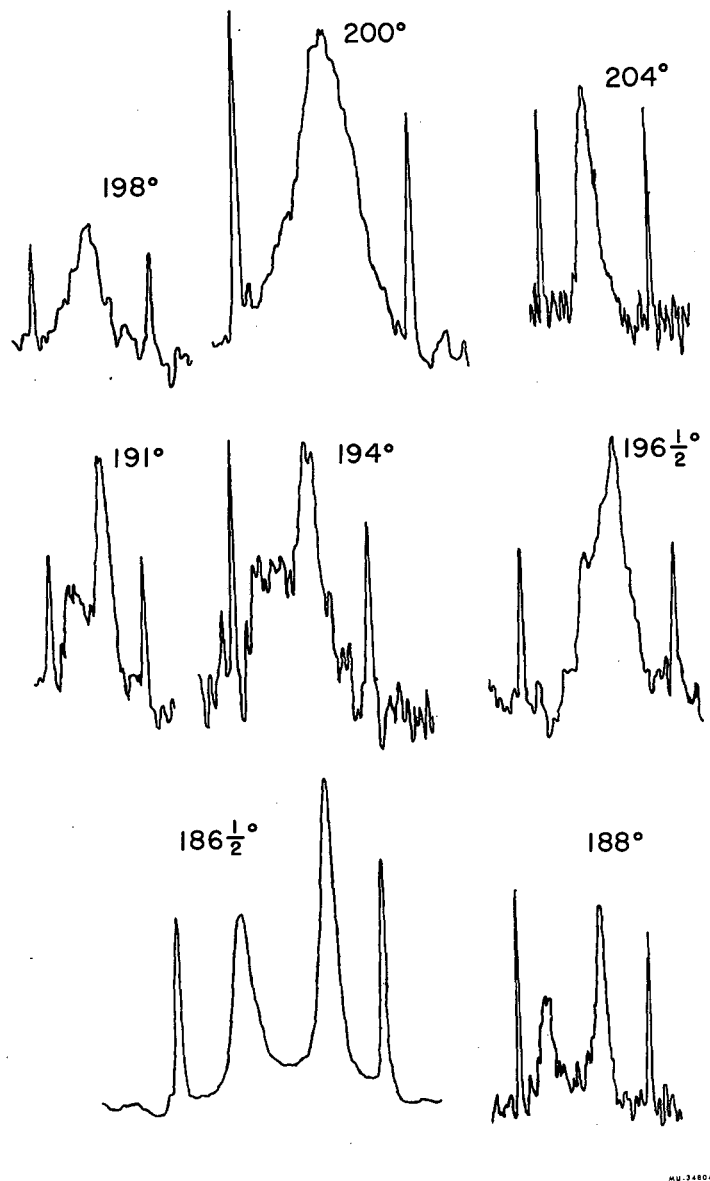
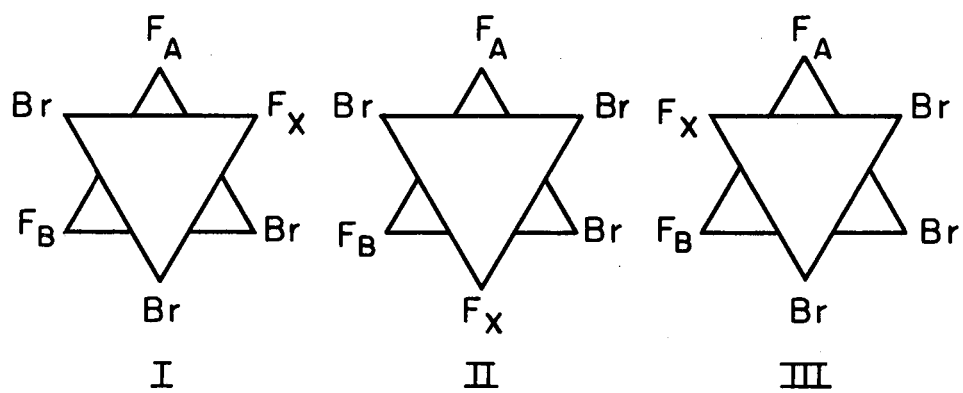
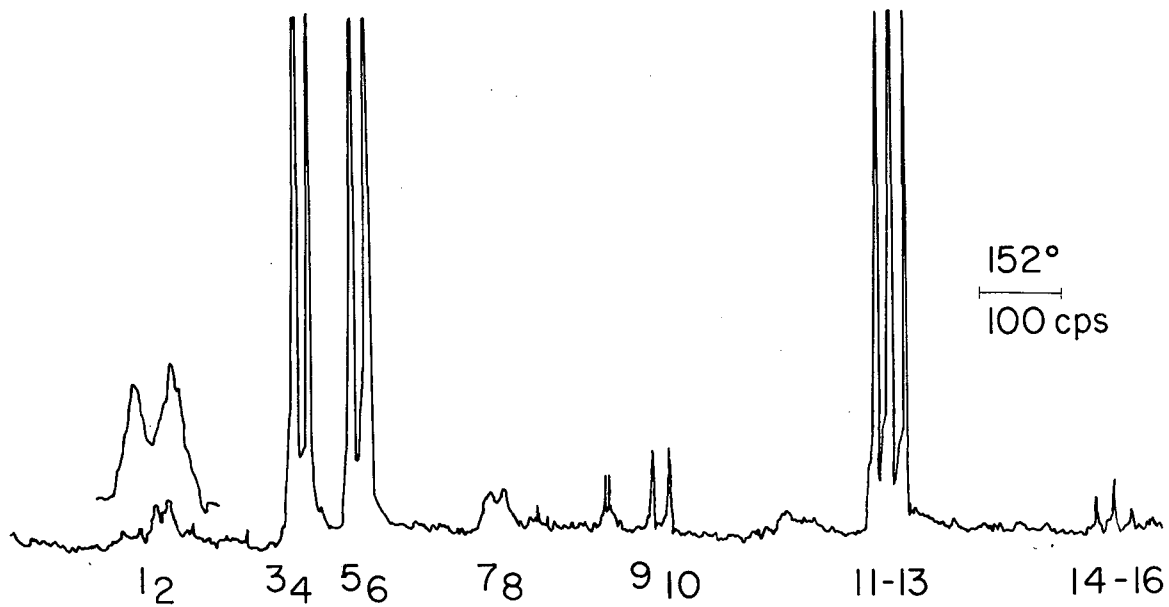


Fig. 9



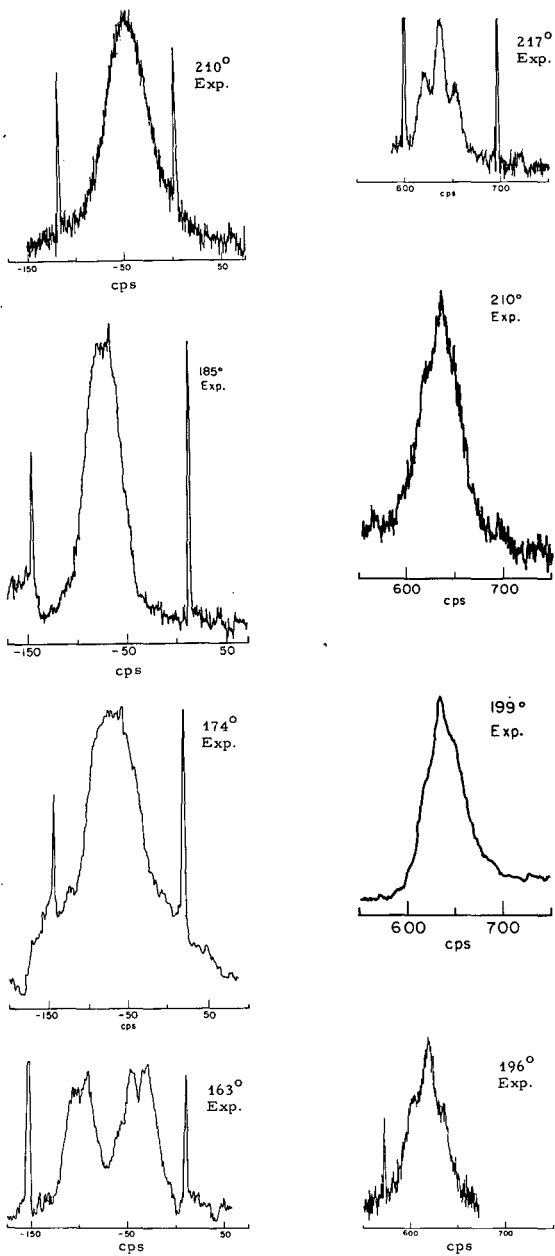
MU-34820

Fig. 10



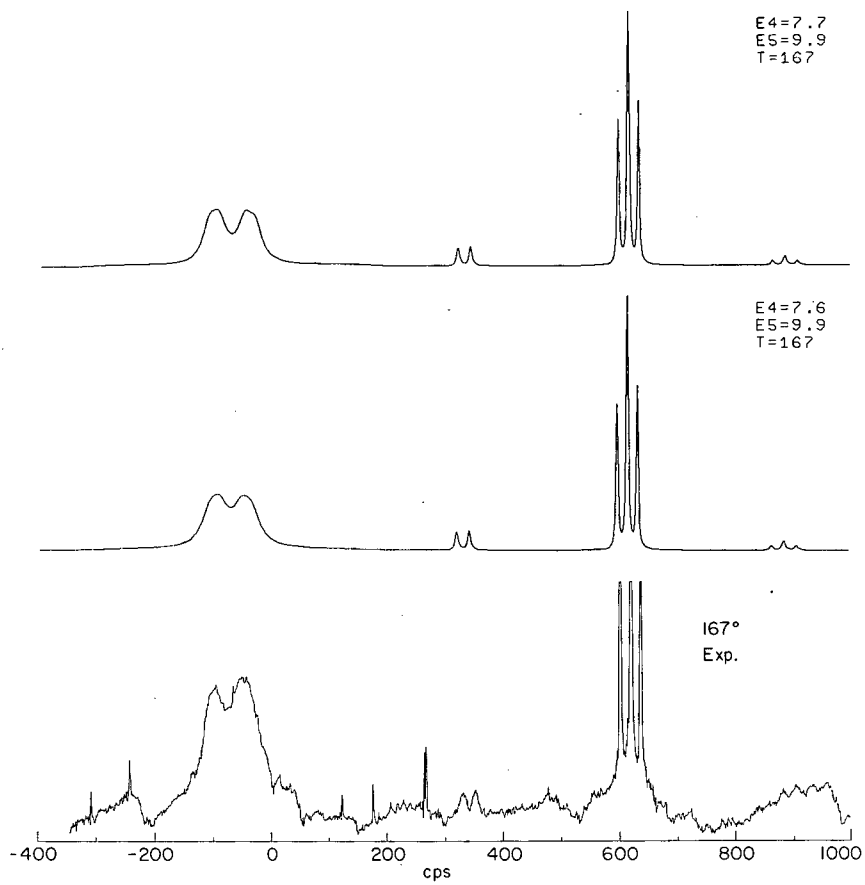
MU-35772

Fig. 11



MUB-4371

Fig. 12



MU-34848

Fig. 13



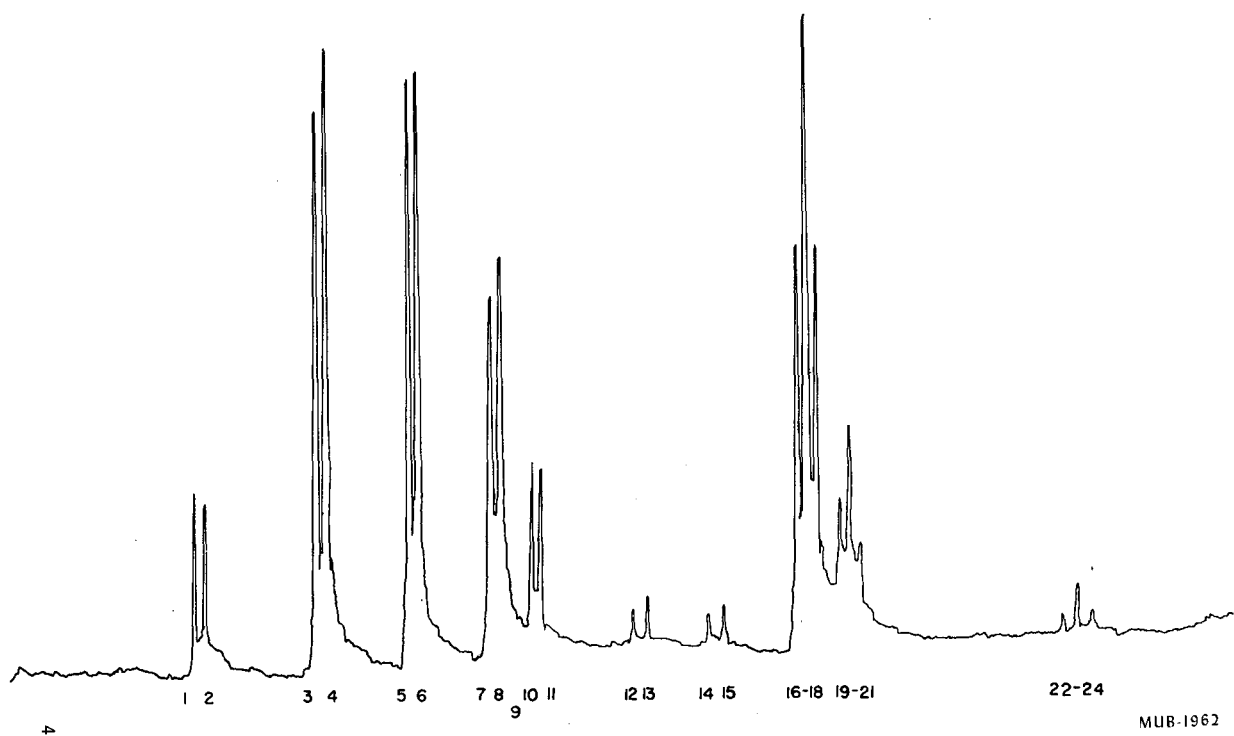
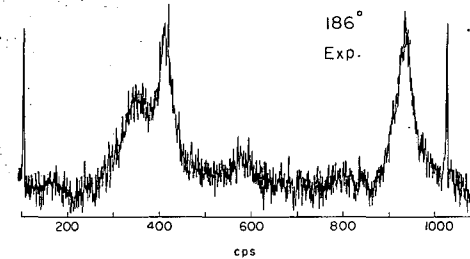
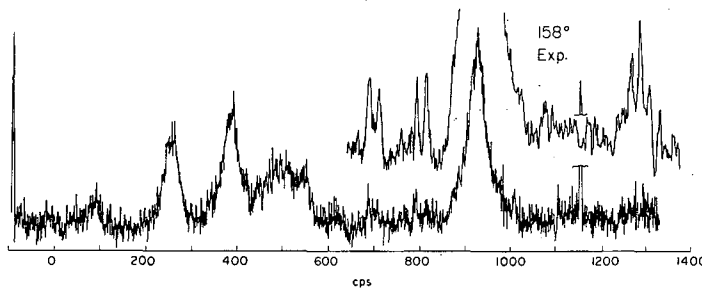
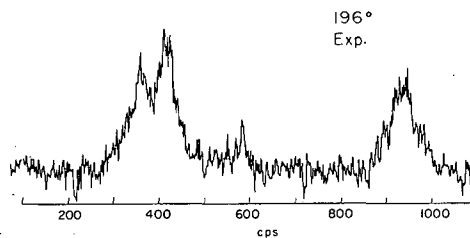
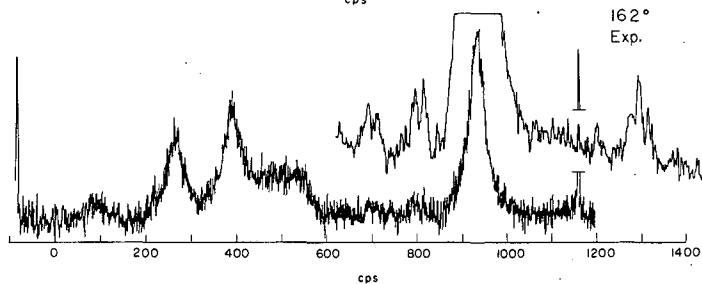
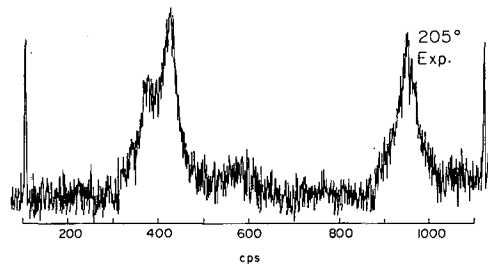
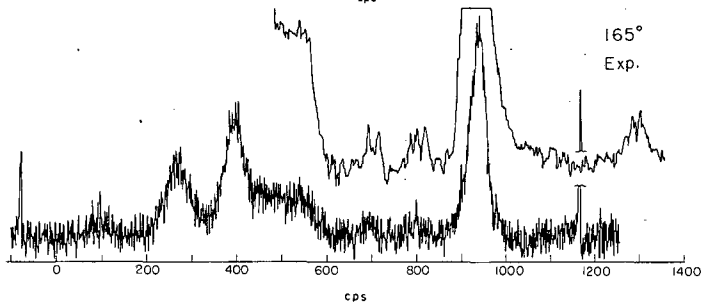
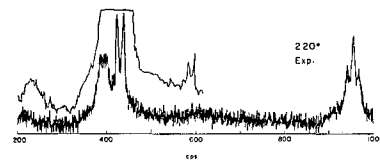
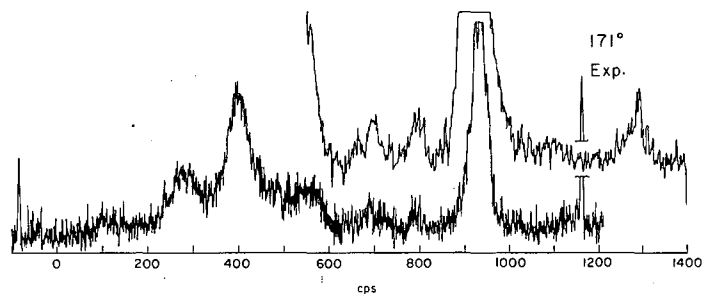
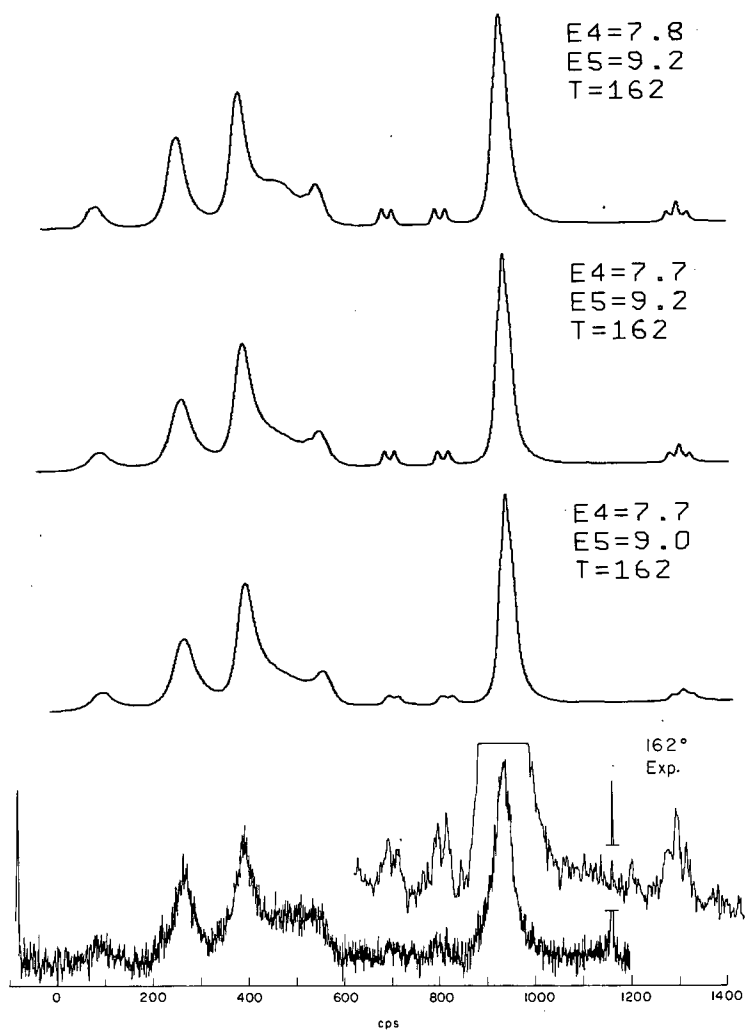


Fig. 14



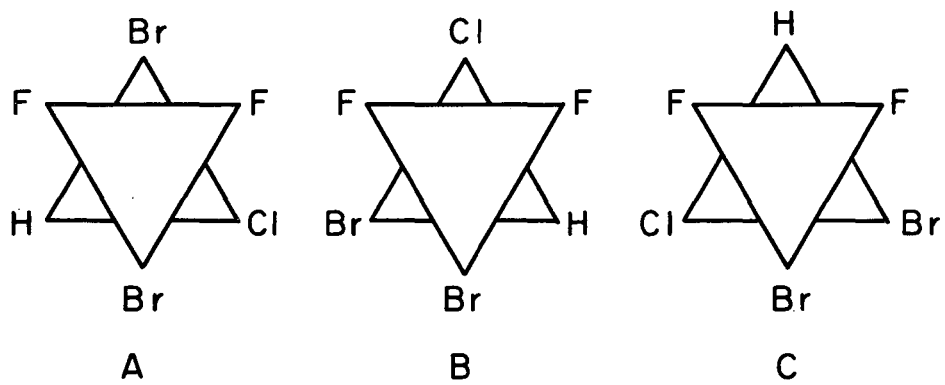
MUB-4407

Fig. 15



MU.34870

Fig. 16



MU-34822

Fig. 21

This report was prepared as an account of Government sponsored work. Neither the United States, nor the Commission, nor any person acting on behalf of the Commission:

- A. Makes any warranty or representation, expressed or implied, with respect to the accuracy, completeness, or usefulness of the information contained in this report, or that the use of any information, apparatus, method, or process disclosed in this report may not infringe privately owned rights; or
- B. Assumes any liabilities with respect to the use of, or for damages resulting from the use of any information, apparatus, method, or process disclosed in this report.

As used in the above, "person acting on behalf of the Commission" includes any employee or contractor of the Commission, or employee of such contractor, to the extent that such employee or contractor of the Commission, or employee of such contractor prepares, disseminates, or provides access to, any information pursuant to his employment or contract with the Commission, or his employment with such contractor.

